

1 **Title Page**

2 **The maize *Hairy Sheath Frayed1 (Hsf1)* mutant alters leaf patterning through**
3 **increased cytokinin signaling**

4

5 **Author names and affiliations**

6 Michael G. Muszynski, ^{a,1} Lindsay Moss-Taylor, ^{b,2} Sivanandan Chudalayandi, ^b James
7 Cahill, ^b Angel R. Del Valle-Echevarria, ^a Ignacio Alvarez, ^c Abby Petefish, ^b Nobue
8 Makita, ^d Hitoshi Sakakibara, ^d Dmitry M. Krivosheev, ^{e,3} Sergey N. Lomin, ^e Georgy A.
9 Romanov, ^e Subbiah Thamocharan, ^f Thao Dam, ^g Bailin Li, ^g and Norbert Brugière ^h

10 ^a Department of Tropical Plant and Soil Sciences, University of Hawai'i at Mānoa,
11 Honolulu, HI 96822, USA.

12 ^b Department of Genetics, Development and Cell Biology, Iowa State University, Ames,
13 Iowa, 50011

14 ^c Department of Statistics, Iowa State University, Ames IA, 50011

15 ^d RIKEN Center for Sustainable Resource Science, Tsurumi, Yokohama 230-0045,
16 Japan.

17 ^e Institute of Plant Physiology; Russian Academy of Sciences, Moscow, 119992, Russia

18 ^f School of Chemical and Biotechnology, SASTRA University; Thanjavur, 613401, India

19 ^g DuPont Crop Genetics, Wilmington, DE 19880

20 ^h DuPont Pioneer, Johnston, IA 50131

21 ORCID IDs: 0000-0002-0817-7594 (M.G.M.);

22

23 ¹ Address correspondence to mgmuszyn@hawaii.edu.

24 ² Present address: Department of Genetics Cell Biology and Development, University of
25 Minnesota, Minneapolis, MN 55455, USA

26 ³ Present address: Vologda State University, Vologda 160000, Russia

27

28 Short Title: Cytokinin influences leaf development

29

30 The author responsible for distribution of materials integral to the findings presented in
31 this article in accordance with the policy described in the Instructions for Authors
32 (www.plantcell.org) is: Michael G. Muszynski (mgmuszyn@hawaii.edu).

33

34 Summary: Increased cytokinin signaling in the maize *Hairy Sheath Frayed1* mutant
35 modifies leaf development leading to changes in patterning, growth and cell identity.

36

37

38 **ABSTRACT**

39 **Leaf morphogenesis requires growth polarized along three axes - proximal-distal,**
40 **medial-lateral and abaxial-adaxial. Grass leaves display a prominent proximal-**
41 **distal (P-D) polarity consisting of a proximal sheath separated from the distal**
42 **blade by the auricle and ligule. Although proper specification of the four**
43 **segments is essential for normal morphology, our knowledge is incomplete**
44 **regarding the mechanisms which influence P-D specification in monocots like**
45 **maize (*Zea mays*). Here we report the identification of the gene underlying the**
46 **semi-dominant, leaf patterning, maize mutant *Hairy Sheath Frayed1* (*Hsf1*). *Hsf1***
47 **plants produce leaves with outgrowths consisting of proximal segments –**
48 **sheath, auricle and ligule – emanating from the distal blade margin. Analysis of**
49 **three independent *Hsf1* alleles revealed gain-of-function missense mutations in**
50 **the ligand binding domain of the maize cytokinin (CK) receptor *Zea mays***
51 ***Histidine Kinase1* (*ZmHK1*) gene. Biochemical analysis and structural modeling**
52 **suggest the mutated residues near the CK binding pocket affect CK binding**
53 **affinity. Treatment of wild type seedlings with exogenous CK phenocopied the**
54 ***Hsf1* leaf phenotypes. Results from expression and epistatic analyses indicated**
55 **the *Hsf1* mutant receptor is expressed normally but appears hypersignaling. Our**
56 **results demonstrate that hypersignaling of CK in incipient leaf primordia can**
57 **reprogram developmental patterns in maize.**

58

59 **INTRODUCTION**

60 Proper leaf morphogenesis in higher plants requires defined patterns of growth
61 polarized along three axes: adaxial-abaxial, medial-lateral and proximal-distal
62 (McConnell and Barton, 1998; Tsukaya, 1998; Bowman et al., 2002; Byrne et al., 2002).
63 Growth along the proximal-distal (P-D) axis is particularly evident in grass leaves, like
64 maize, which are composed of four distinct segments; the sheath is proximal, the blade

65 is distal and the auricle and ligule form the boundary between the two (Figure 1A)
66 (Sylvester et al., 1996). A number of genes have been identified that influence P-D
67 patterning, with *BLADE-ON-PETIOLE (BOP)* genes affecting proximal identity in
68 eudicots and monocots (Ha et al., 2003, 2004; Norberg et al., 2005; Toriba et al., 2019;
69 Moon et al., 2013; Tavakol et al., 2015). In grasses, ectopic expression of class I
70 *knotted1like homeobox (knox)* transcription factor genes in developing leaf primordia
71 alters P-D patterning, primarily disrupting the formation of a defined sheath-blade
72 boundary (Freeling and Hake, 1985; Hake et al., 1989, 1991; Smith et al., 1992;
73 Schneeberger et al., 1995; Muehlbauer et al., 1997; Foster et al., 1999a; Tsiantis et al.,
74 1999; Byrne et al., 2001). Class I *knox* genes typically function in meristem formation
75 and maintenance, and their down-regulation is required for normal development of
76 determinant organs like leaves (Endrizzi et al., 1996; Long et al., 1996; Kerstetter et al.,
77 1994). In meristems, KNOX proteins function to increase cytokinin (CK) accumulation
78 by positive regulation of CK synthesis genes and simultaneously decrease gibberellic
79 acid (GA) accumulation by suppression of GA biosynthesis genes or activation of GA
80 catabolic genes (Ori et al., 2000; Sakamoto et al., 2001; Hay et al., 2002; Jasinski et al.,
81 2005; Yanai et al., 2005; Sakamoto et al., 2006; Bolduc and Hake, 2009). Recently, a
82 rice KNOX transcription factor was shown to also affect brassinosteroid (BR)
83 accumulation by upregulating BR catabolism in the shoot apical meristem (Tsuda et al.,
84 2014). Determinate leaf primordia form when *knox* expression is down-regulated by the
85 action of ROUGH SHEATH2 (RS2) and related proteins resulting in a decrease in CK
86 and increase in GA accumulation (Hay et al., 2006; Guo et al., 2008). In addition to the
87 action of CK and GA, auxin is required for proper leaf initiation and positioning. The
88 polar transport of auxin by PINFORMED1 (PIN1) auxin efflux carriers guides the
89 formation of auxin maxima, localized regions of high auxin accumulation, that is
90 required for initiation of leaf primordia (Pozzi et al., 2001; Scarpella et al., 2006;
91 Benjamins and Scheres, 2008; Zhao, 2008). The emerging model predicts that spatial
92 differences in cytokinin/auxin ratios control final cell fate (Shani et al., 2006; Muller and
93 Sheen, 2008). Ectopic *knox* expression presumably shifts critical phytohormone ratios
94 in developing leaf primordia but the exact molecular mechanisms by which
95 phytohormone ratios determine leaf patterning remain incomplete.

96 As phytohormones play pivotal roles in many developmental programs, the
97 pathways that signal their perception and response have been well characterized. For
98 example, the perception and response to the CK phytohormones relies on a two-
99 component signal transduction system (Hwang and Sheen, 2001; Yonekura-Sakakibara
100 et al., 2004; Hwang and Sakakibara, 2006; Du et al., 2007; To and Kieber, 2008). The
101 perception of CK is mediated via a partially redundant signaling system of histidine
102 kinases (HKs), histidine phosphotransfer proteins (HPTs) and response regulators
103 (RRs). CK signaling begins with the perception of CK by binding to HK receptors at the
104 ER, and probably also plasma membrane, which triggers receptor phosphorylation
105 (Lomin et al., 2011). The activated receptors initiate phosphorelay by transferring
106 phosphoryl groups to HPTs, which shuttle between the cytoplasm and nucleus. Once in
107 the nucleus, phosphorylated HPTs transfer their phosphoryl groups to type-B RRs,
108 which in turn activate expression of type-A RRs and other CK responsive genes
109 (Rashotte et al., 2006). The type-A RRs and other CK-responsive genes mediate
110 several CK-regulated processes including shoot and root growth, de-etiolation, leaf
111 expansion, root vascular development, senescence, and cytokinin homeostasis (To and
112 Kieber, 2008). In maize, multiple members of each of the CK signaling components
113 have been identified (Yonekura-Sakakibara et al., 2004). Maize has seven HKs
114 (ZmHKs) of which three have been shown to bind and signal various types of CKs in
115 heterologous assays (Lomin et al., 2011; Steklov et al., 2013). Three HPTs (ZmHPs),
116 three type-B RRs and seven type-A RRs (ZmRRs) have also been identified in maize
117 (Asakura et al., 2003). Of these signal transduction components, the function of only
118 *ZmRR3*, a type-A RR, has been defined by null mutations and shown to underlie the
119 *aberrant phyllotaxy1 (abph1)* mutation (Jackson and Hake, 1999; Giulini et al., 2004).
120 Our understanding of the functions of other components of the CK signal transduction
121 pathway remains largely incomplete for cereal species like maize.

122 To gain a better understanding of the signaling mechanisms which mediate leaf
123 pattern specification, we initiated a study of the semi-dominant *Hairy Sheath Frayed1*
124 (*Hsf1*) mutation which alters P-D leaf development in maize (Bertrand-Garcia and
125 Freeling, 1991a). Although *Hsf1* disrupts the P-D leaf pattern similar to dominant class I

126 *knox* mutations, *Hsf1* is not itself a *knox* gene, since it does not map to the location of
127 any maize *knox* genes (Bertrand-Garcia and Freeling, 1991b). In this report, we show
128 that the *Hsf1* phenotype results from specific missense mutations in the maize CK
129 receptor *Zea mays Histidine Kinase1 (ZmHK1)* gene (Yonekura-Sakakibara et al.,
130 2004). Our analyses of mutant receptor function, the effects of exogenous CK
131 treatment on leaf development, and epistatic interaction suggest that the ZmHK1
132 receptor is hypersignaling in *Hsf1* mutants. Overall, our results indicate CK
133 hypersignaling can influence the specification of P-D leaf patterning in maize and
134 underscores the capacity of CK to alter developmental programs.

135

136 **RESULTS**

137 **The *Hsf1* mutation induces specific alterations to maize leaf patterning**

138 The original *Hsf1* mutation arose via ethyl methanesulfonate (EMS) mutagenesis of the
139 inbred line Mo17 and was designated *Hsf1-N1595* (also called *Hsf1-O*) (Bird and
140 Neuffer, 1985). A second mutation, *Hsf1-N1603* (hereafter called *Hsf1-1603*), was
141 shown to be allelic or very closely linked (Bertrand-Garcia and Freeling, 1991a). We
142 isolated three additional alleles in independent EMS mutagenesis screens in different
143 inbred backgrounds: *Hsf1-AEWL* in A619, *Hsf1-2559* in Mo17, and *Hsf1-7322* in A632.
144 All *Hsf1* alleles have very similar phenotypes compared to the *Hsf1-N1595* (hereafter
145 called *Hsf1-1595*) reference mutation. As was shown previously for *Hsf1-1595*, plants
146 heterozygous for any of the *Hsf1* alleles display a highly penetrant mutant leaf
147 patterning phenotype with outgrowths consisting of sheath, auricle and ligule emanating
148 from the distal blade margin (Figures A -1C) (Bertrand-Garcia and Freeling, 1991a).
149 The outgrowths have proximal identity, were termed “prongs”, and we adopted this term
150 to describe this structure (Figure 1B). Although *Hsf1* mutant plants have proximal tissue
151 growing on the distal blade, they have a normal blade-sheath boundary (Figure 1A)
152 (Bertrand-Garcia and Freeling, 1991a). All the pleiotropic phenotypes described for
153 *Hsf1-1595* in Bertrand-Garcia and Freeling (1991a) are shared by all the other *Hsf1*

154 alleles, including an increase in macrohair size and density on the abaxial sheath,
155 adaxial blade, and blade margin, an increase in leaf number, shorter stature, short and
156 narrow leaves, and reduced root growth (Supplemental Figures 1A and 1B;
157 Supplemental Table 1). Bertrand-Garcia and Freeling (1991a) also showed
158 homozygous *Hsf1* plants have a stronger mutant phenotype being extremely stunted,
159 with multiple shoots arising from the coleoptile node at germination, and having
160 adventitious needle- or club-shaped leaves (Supplemental Figures 1A and 1B).

161 Since plants heterozygous for either *Hsf1-1595*, *Hsf1-1603*, or *Hsf1-AEWL* were
162 phenotypically very similar (Figure 1C), we chose the *Hsf1-1603* allele to characterize
163 the temporal and spatial patterns of prong formation to better understand how the *Hsf1*
164 mutation affected leaf patterning. In *Hsf1-1603* heterozygotes, prongs first appeared on
165 leaf 5 in a few plants, and most commonly appeared on leaf 6 or leaf 7 but never on
166 earlier arising leaves (Supplemental Figure 1C). The earliest sign of P-D leaf polarity
167 specification is the formation of the preligule band (PLB) which will differentiate into the
168 auricle and ligule (Sylvester et al., 1990; Johnston et al., 2014). Formation of the PLB
169 typically is first observed in plastochron 5 or 6 stage leaf primordia (P5- P6) with the
170 initiating ligule becoming visible about plastochron 7 or 8 (P7-P8) (Johnston et al.,
171 2014). Plastochron describes the stage of leaf primordia development and refers to the
172 position of the primordia relative to the shoot apical meristem (SAM) (Sylvester et al.,
173 1990). Thus, a P5 primordium has four younger primordia between it and the SAM. To
174 determine if the *Hsf1-1603* mutation influenced the timing of the acquisition of P-D
175 polarity, we examined leaf primordia in *Hsf1-1603/+* and wild type sib plants for signs of
176 early ligule development (see Methods). The initiating ligule was most commonly first
177 visible on P7 primordia in both wild type and *Hsf1-1603* heterozygotes indicating no
178 influence on P-D polarity acquisition (Supplemental Figure 1E). To determine if the
179 appearance of prong primordia on the blade margin coincided with the acquisition of P-
180 D polarity, developing leaf primordia from *Hsf1-1603* heterozygotes were dissected and
181 examined for the presence of initiating prongs. Prong initials were most commonly
182 observed on the blade margins of P5 or P6 leaf primordia but some were noted as early
183 as P4 (Supplemental Figure 1D, 1F to 1G), consistent with prong formation in *Hsf1-*

184 1595 heterozygotes (Bertrand-Garcia and Freeling, 1991b). Thus prongs typically
185 initiated from blade margins about the same plastochron stage as formation of the PLB.

186 Prongs were observed to occur in different sizes and at different positions along
187 the leaf blade margin (Figures 1B and 1F and Supplemental Figure 2A). To determine if
188 prong formation was random or patterned, we measured the size and position of each
189 prong from both margins of mature leaves collected from different positions on the shoot
190 of *Hsf1-1595*, *Hsf1-1603* and *Hsf1-AEWL* heterozygous plants. Results showed that
191 prong formation was more frequent on leaves higher on the shoot (Supplemental Table
192 2) with prongs occupying more of the blade margin in these upper leaves compared to
193 lower leaves (Supplemental Figures 2B and 2C). Next we determined where prongs
194 formed along the P-D axis of the blade. Analysis indicated prongs only formed in the
195 proximal 70% and never in the distal 30% of the blade, with the majority of prongs
196 forming within a region encompassing the proximal 15% – 40% of the blade
197 (Supplemental Figure 2D). Next we examined the range of prong sizes for each *Hsf1*
198 allele within this prong-forming region. For all three alleles, the majority of prongs were
199 about a centimeter in size but a few were larger, ranging from 3 – 6 centimeters
200 (Supplemental Figure 2E). With relative position and size known, we next asked
201 whether prong position was related to its size. In general, the largest prongs often
202 formed in the basal 20% of the blade and smaller prongs formed at any position within
203 the prong forming region (Supplemental Figure 2F). Thus, our analysis indicated prong
204 formation was not random but occurred in particular regions of the blade and initiated at
205 specific developmental stages.

206

207 **Gain-of-function mutations in the maize cytokinin receptor gene *ZmHK1* underlie** 208 **the *Hsf1* mutation**

209 Previous studies mapped *Hsf1-1595* to the long arm of chromosome 5 (Bertrand-Garcia
210 and Freeling, 1991b). To isolate the gene underlying the *Hsf1* locus, we screened a
211 backcross mapping population of over 3,000 plants with linked molecular markers

212 derived from the maize reference genome (B73 RefGen_v1). The *Hsf1* locus was
213 localized to a 21-kb interval with a single gene model (GRMZM2G151223, B73
214 RefGen_v2). This gene model was well supported with abundant EST evidence and
215 was annotated as encoding *Zea mays Histidine Kinase1 (ZmHK1)*, one of seven maize
216 histidine kinase cytokinin receptors (Supplemental Figure 3) (Yonekura-Sakakibara et
217 al., 2004; Steklov et al., 2013). To confirm *ZmHK1* was the correct gene and to identify
218 the causative lesions, the *ZmHK1* gene was sequenced from all five *Hsf1* alleles. The
219 entire *ZmHK1* genomic region, including ca. 2-kb upstream and downstream of the
220 transcription start and stop, was sequenced from *Hsf1-1595*, *Hsf1-1603*, *Hsf1-2559*,
221 *Hsf1-7322* and *Hsf1-AEWL* homozygotes and their progenitor inbred lines. As expected
222 for EMS-generated mutations, single nucleotide transitions were identified in the five
223 *Hsf1* alleles compared to their progenitor sequences. Although each allele arose
224 independently, *Hsf1-1595* and *Hsf1-1603* had the exact same transition mutations as
225 *Hsf1-7322* and *Hsf1-2559*, respectively. Thus, hereafter, we refer to the three different
226 *Hsf1* alleles: *Hsf1-1595*, *Hsf1-1603* and *Hsf1-AEWL*. Each transition mutation produced
227 a missense mutation in a highly conserved amino acid located in the CHASE
228 (cyclases/histidine-kinase-associated sensory) domain of the ZmHK1 protein, where CK
229 binding occurs (Figure 1H) (Hothorn et al., 2011; Steklov et al., 2013). The *Hsf1-1595*
230 mutation changed proline 190 to leucine (CCA>CTA), the *Hsf1-1603* mutation changed
231 glutamate 236 to lysine (GAG>AAG), and the *Hsf1-AEWL* mutation changed leucine
232 238 to phenylalanine (CTT>TTT). The missense mutation in *Hsf1-AEWL* is particularly
233 significant because this is the same type of amino acid substitution, although at a
234 slightly different position in the CHASE domain, which was found in another gain-of-
235 function mutation in a CK receptor, the *spontaneous nodule formation2 (snf2)* mutation
236 in the lotus *Lhk1* receptor, (Figure 1D) (Tirichine et al., 2007). The *snf2* mutation was
237 shown to cause mutant LHK1 to signal independent of the CK ligand in a heterologous
238 signaling assay suggesting the *snf2* mutation locked LHK1 in an active signaling state
239 (Tirichine et al., 2007). Based on the location and nature of the amino acid substitutions
240 in the three *Hsf1* mutations and the presumed mode of action of the *snf2* mutation in
241 *Lhk1*, we hypothesized that the *Hsf1* mutations might also lock the ZmHK1 receptor in
242 an active CK signaling state and signal independent of CK.

243

244 **The *Hsf1* mutant CK receptors have altered histidine kinase signaling and ligand**
245 **binding activities**

246 To determine if the *Hsf1* mutant receptors are signaling independent of CK, we utilized
247 a heterologous histidine kinase signaling assay system developed in the yeast
248 *Saccharomyces cerevisiae* (Suzuki et al., 2001). In the yeast assay, the cognate his-
249 kinase of an endogenous two-component phosphorelay signal transduction system was
250 deleted. Functional replacement of the endogenous his-kinase with the assayed CK
251 receptor, in this case ZmHK1, allowed the activity of the receptor to be determined as
252 the output of the endogenous yeast transduction system, which is the ability to grow on
253 glucose media (Suzuki et al., 2001). We engineered the exact point mutation found in
254 each *Hsf1* mutation into the *ZmHK1* cDNA in the p415CYC-ZmHK1 plasmid for
255 expression in yeast (Suzuki et al., 2002; Higuchi et al., 2009). We next tested receptor
256 activity in the *sln1* deletion yeast strain TM182 carrying each of the *Hsf1* missense
257 mutations, the wild type *ZmHK1* cDNA, and the empty p415CYC vector grown on
258 glucose media with and without the CK ligand (Figure E). As expected, the wild type
259 ZmHK1 strain only grew well on glucose media supplemented with higher
260 concentrations of the three CKs tested (Figure 1E) and, at lower CK concentrations,
261 only grew robustly on glucose with the preferred ligand *N*⁶-(Δ^2 -isopentenyl) adenine (iP)
262 (Supplemental Figures 3A to 4C). In the absence of added CK, strains carrying either
263 ZmHK1-AEWL or ZmHK1-1603 grew robustly on glucose media (Figure 1E). This
264 result indicated that the ZmHK1-AEWL and ZmHK1-1603 receptors signaled
265 independent of added CK in this assay. To determine if the mutant receptors were still
266 CK responsive, they were also grown on glucose media supplemented with the three
267 tested CKs (Figure 1E). Growth on glucose supplemented with different CKs did not
268 reveal any receptor activity differences between ZmHK1-AEWL and ZmHK1-1603.
269 Surprisingly, growth of the ZmHK1-1595 strain was different than the two mutant
270 receptors and wild type. The ZmHK1-1595 strain did not grow on glucose media
271 without added CK, similar to wild type ZmHK1 (Figure 1E). Instead, the ZmHK1-1595
272 strain showed strong growth on glucose media with 10 μ M of the preferred CK iP and

273 weaker growth on glucose with 10 μ M of two other bioactive CKs, *trans*-zeatin (tZ) and
274 *cis*-zeatin (cZ), suggesting ZmHK1-1595 had weak receptor activity in this assay (Figure
275 1E

276

277 To investigate ligand specificity differences, CK ligand binding affinities were
278 determined for the mutant and wild type receptors (Romanov et al., 2005; Lomin et al.,
279 2011). Affinities were determined for 6 different CKs and adenine (Ade) using two
280 binding assays with receptors expressed in bacterial spheroplasts (Romanov et al.,
281 2005) or residing in tobacco membranes after transient expression *in planta* (Lomin et
282 al., 2015, 2011). The ligand preferences for the wild type ZmHK1 receptor were
283 comparable to those determined previously (Table 1) (Lomin et al., 2015, 2011). The
284 mutant receptors, on the other hand, all showed increased affinities for most of the CKs
285 tested (Table 1). The preference ranking of the mutant receptors for different CKs was
286 mostly similar to wild type (Supplemental Figure 4) but the affinities were increased
287 between 2- to 8-fold (Table 2). The only exception was the affinity for the synthetic CK
288 thidiazuron, which was reduced for all the mutant receptors compared to wild type
289 ZmHK1. Thus, the missense mutations in the *Hsf1* alleles increased the relative binding
290 affinity of the receptor for all the natural CKs tested, suggesting the mutant receptors
291 might be hypersignaling.

292

293 **The *Hsf1* missense mutations localize near the CK binding pocket in ZmHK1**

294 To gain better insight into how each *Hsf1* missense mutation might impact CK binding,
295 we determined the effect these mutations had on the structure of the CHASE domain,
296 which was facilitated by the publication of the crystal structure of the *Arabidopsis*
297 *thaliana histidine kinase4 (AHK4)* gene CHASE domain (Hothorn et al., 2011). *AHK4* is
298 co-orthologous to *ZmHK1* and three other paralogous histidine kinases in the maize
299 genome (Steklov et al., 2013). To explore the effects of the *Hsf1* mutations on receptor
300 structure, homology modeling was used first to model the 3D structure of the CHASE

301 domain of ZmHK1 using the structure of AHK4. This was done with and without CK
302 occupying the binding pocket, which did not change the results. Given the high degree
303 of amino acid identity between ZmHK1 and AHK4, the ZmHK1 CHASE domain
304 structure was resolved with high confidence. Next, each mutant receptor was modeled
305 based on the derived ZmHK1 structure. The models were subjected to dynamics
306 simulation with appropriate solvation (see Methods). The results of homology modeling
307 showed that the amino acids mutated in each *Hsf1* allele do not occur within the CK
308 binding pocket (Figure 1F) and thus do not contribute to direct polar contacts with the
309 ligand. Instead, each altered residue is located near a loop domain that forms one face
310 of the binding cavity. An indication of how the mutated residues at these positions
311 might affect ligand binding was provided by the structure model of the ZmHK1-1603
312 receptor. The residue altered in ZmHK1-1603 is E236, which is predicted to form an
313 ion-pair interaction with R192 located in the loop domain. This polar interaction may
314 help to stabilize the position of the loop domain (Figure 1F). The *Hsf1-1603* mutation
315 converts E236 to K, a negative to positive residue change, which is expected to break
316 the polar interaction with R192 and possibly destabilize the position of the loop due to
317 the nearness of the two positively charged residues. Altering the position of the loop
318 may change the overall conformation of the ligand binding pocket and, thus, account for
319 differences in ligand binding affinities. The missense residues in the other two mutant
320 receptors could potentially alter the conformation of the CK binding pocket via a
321 different mechanism, although our modeling results did not reveal an obvious one.

322 **Exogenous CK treatment recapitulated the *Hsf1* phenotype**

323 The biochemical and structural analyses suggested the *Hsf1* mutant receptor might be
324 hypersignaling the perception of CK which altered leaf development. To test the idea
325 that increased CK signaling could produce *Hsf1*-like phenotypes, wild type, B73 inbred
326 seeds were transiently treated with the CK 6-benzylaminopurine (6-BAP). The embryo
327 in a mature maize seed possesses about 5 leaf primordia and it is these primordia
328 which experienced the hormone treatment (Kerstetter and Poethig, 1998). Imbibed
329 seeds were treated for 6 days with 10 μ M 6-BAP, rinsed and transplanted to soil (see
330 Methods). After growth for 3-weeks, the first 4 seedling leaves were examined for

331 developmental changes (Figures 2A to 2E). Similar to *Hsf1*, 100% of the CK treated
332 B73 seeds produced smaller seedling leaves covered with abundant macrohairs
333 (Figures 2A to 2E). Leaf sheath length, blade length and blade width were reduced by
334 10% - 20% for leaf 3, similar to leaf size reductions in the *Hsf1* seedlings (Figure 2C).
335 In addition, macrohair density increased on the abaxial sheath, near the auricle, on the
336 adaxial blade, and blade margins in 100% of the CK-treated B73 seedlings (Figures 2D
337 and 2E). This pattern of ectopic macrohair formation was similar to that seen in *Hsf1*
338 seedlings (Bertrand-Garcia and Freeling, 1991a). In addition to alterations in leaf size
339 and pubescence, nearly 20% of the CK treated B73 seeds produced seedlings with
340 prongs on leaf 4 (Figures 2F). This was in contrast to *Hsf1* seedlings where prongs
341 rarely, if ever, developed on leaf 4 (Supplemental Figure 1C). Increasing the
342 concentration of exogenous 6-BAP to 100 μ M increased the number of B73 seedlings
343 with prongs on leaf 4 to nearly 90%. (Figure 2F) Thus, transient, exogenous CK
344 treatment recapitulated three prominent aspects of the *Hsf1* phenotype: reduced leaf
345 size, increased macrohair abundance, and formation of prongs on blade margins,
346 confirming these developmental changes can be induced by CK.

347 If CK hypersignaling in *Hsf1* was due to increased ligand affinity, then we would
348 expect *Hsf1* to be hypersensitive to CK treatment. To test this idea, we performed six-
349 day treatments on segregating *Hsf1-1603/+* seeds using 0.1 μ M CK, a concentration
350 that did not elicit leaf size changes in B73 inbred seed (Supplemental Figure 5A). To
351 distinguish segregating heterozygous *Hsf1* plants from wild type sib plants, PCR
352 genotyping was used to detect a size polymorphism in the *Hsf1-1603* allele
353 (Supplemental Table 3). After CK treatment, seedlings were grown for 3 weeks, after
354 which, leaf phenotypes were measured. While 0.1 μ M CK treatment had no effect on
355 wild type sibling leaf size (Supplemental Figure 5A), it did reduce the leaf size of *Hsf1-1603/+*
356 plants 10% - 30% (Supplemental Figure 5B). Thus, *Hsf1-1603/+* seedlings were
357 responsive to a lower concentration of CK that did not elicit a response in wild type sib
358 or B73 inbred seedlings. Treatment with 10 μ M 6-BAP was also used to assess effects
359 on prong and macrohair formation in *Hsf1-1603/+* plants. Similar to earlier results
360 (Supplemental Figure 1C), seedlings from control water-treated *Hsf1-1603/+* seeds first

361 formed prongs on leaf 5 (ca. 5%) or leaf 6 (ca. 25%) but never on earlier arising leaves
362 (Figure 2G to 2I). In fact, about 60% of *Hsf1-1603/+* seedlings normally first formed
363 prongs on leaves arising on or after leaf 7 (Figure 2H). By contrast, of the 10 μ M 6-BAP
364 treated *Hsf1-1603/+* seeds, nearly 60% produced seedlings where prongs first formed
365 on leaf 4 and only about 30% formed prongs on leaves arising on or after leaf 7 (Figures
366 2G to 2I). In addition, macrohair abundance appeared increased for CK-treated *Hsf1-*
367 *1603/+* compared to control *Hsf1-1603/+* or 6-BAP treated wild type sib seedlings but
368 this was not measured (Figure 2J). Thus, CK treatment of *Hsf1* resulted in earlier
369 arising and enhanced mutant phenotypes, indicating the mutation was hypersensitive to
370 the CK hormone, consistent with the biochemical analysis of the receptor.

371

372 **CK responsive genes are up-regulated in *Hsf1* leaf primordia**

373 Based on the *Hsf1* mutant plant phenotypes, we presumed that hypersignaling in
374 developing leaf primordia gave rise to the alterations in P-D leaf patterning and other
375 phenotypes. To test this idea, we determined the expression of *ZmHK1* and several CK
376 responsive genes in *Hsf1-1603/+* and wild type sibling plants. Published qPCR and *in*
377 *silico* expression analyses
378 (https://www.maizegdb.org/gene_center/gene/Zm00001d017977#rnaseq) indicated
379 *ZmHK1* was expressed broadly across several tissues including leaves, roots, stem,
380 and tassel (Yonekura-Sakakibara et al., 2004). We reverse transcribed cDNA from
381 three tissues, shoot apices (shoot apical meristem plus 3 youngest leaf primordia),
382 immature leaf, and mature green leaf from two-week old seedlings. Using quantitative
383 PCR (qPCR) we assessed expression in plants heterozygous for the three *Hsf1* alleles
384 compared to their wild type sibs (Figure 3A). We did not detect an increase in *ZmHK1*
385 transcript accumulation in the *Hsf1/+* mutants compared to their wild type controls.
386 Next, we examined expression of CK-responsive genes; two type-A response
387 regulators, *ZmRR3* and *ZmRR6*, and a cytokinin oxidase gene, *ZmCKO4b* (Asakura et
388 al., 2003; Giulini et al., 2004). We found increased transcript accumulation for all three

389 CK-responsive genes in the *Hsf1/+* mutants, although there was some inconsistencies
390 across genotypes and tissues (Figure 3A).

391 Using *in situ* hybridization, we assessed transcript localization of *ZmHK1* and
392 *ZmRR3* in wild type and *Hsf1-1603/+* shoot apices (Figure 3B). . The *ZmHK1* transcript
393 was found to be distributed broadly within developing leaf primordia and shoot apices in
394 both genotypes (Figure 3B). As was demonstrated previously, *ZmRR3* was expressed
395 in a specific wedge-shaped domain in the apical meristem in both longitudinal and
396 transverse sections of wild type apices but no signal was detected in leaf primordia
397 (Figure 3B) (Giulini et al., 2004). . However, the spatial expression of *ZmRR3* was
398 expanded in *Hsf1-1603/+* apices Strong *ZmRR3* expression was visible in its normal
399 meristem domain but signal was also detected in leaf primordia and was particularly
400 evident at the margins (Figure 3B) Given the expanded pattern of *ZmRR3* expression
401 in *Hsf1-1603/+* leaf primordia margins and that *ZmRR3* expression is CK responsive,
402 we interpreted this to indicate increased CK signaling in in the tissue where prongs will
403 form.

404

405 **Mutation of *ZmRR3*, a negative regulator of CK signaling, enhances the *Hsf1*** 406 **phenotype**

407 To test if the increased transcript accumulation of the CK responsive genes was
408 biologically relevant, we made use of a null allele of *ZmRR3*, also known as *aberrant*
409 *phyllotaxy1* (*abph1*). Plants homozygous for the recessive *abph1* reference allele have
410 an altered phyllotactic pattern and develop leaves paired 180° at each node instead of
411 having the normal alternating pattern (Figures 4A and 4B) but have no P-D patterning
412 defects (Jackson and Hake, 1999). Backcross families were produced which
413 segregated four phenotypes – wild type, heterozygous *Hsf1-1603*, homozygous *abph1*,
414 and heterozygous *Hsf1-1603* plus homozygous *abph1* – in equal frequencies (Figures
415 4A and 4B). Double mutant plants, heterozygous for *Hsf1* and homozygous for *abph1*,
416 had paired leaf phyllotaxy and a strongly enhanced *Hsf1* phenotype, including very

417 stunted stature, increased shoot branching, slow growth, extremely short and narrow
418 leaves, and severe leaf patterning defects including abundant prongs and bi- or
419 trifurcation of leaf blades (Figure 4B). The synergistic interaction of *Hsf1* and *abph1*
420 was consistent with *ZmRR3* functioning as a negative regulator of CK signaling and
421 indicated the loss of *abph1* function enhanced the *Hsf1* phenotype.

422

423 **DISCUSSION**

424 **CK influences specific developmental programs in maize leaves**

425 In this study we showed that the *Hsf1* mutation conditions a CK hypersignaling
426 phenotype that has multiple effects on plant growth and development, including specific
427 effects on (i) leaf patterning, (ii) leaf size and (iii) leaf epidermal cell fate (Bertrand-
428 Garcia and Freeling, 1991a). Supporting this idea, we also show exogenous CK
429 treatment of wild type maize seeds produced similar changes in these developmental
430 programs. . Prominent among the developmental changes was a specific alteration in
431 P-D leaf patterning where ectopic outgrowths with proximal identity (prongs) formed in
432 the distal blade (Figures 1A to 1C and Supplemental Figure 2A). Although growth along
433 the P-D axis is fundamental to normal leaf development and morphology, its molecular
434 control has not been fully characterized. In eudicots, the activities of several
435 transcription factor genes, such as, *BLADE ON PETIOLE1 (BOP1)*, *LEAFY PETIOLE*
436 (*LEP*), and *JAGGED (JAG)*, have been linked to the control of P-D leaf development
437 (van der Graaff et al., 2000, 2003; Ha et al., 2004; Ohno et al., 2004; Norberg et al.,
438 2005). *BOP* genes have also been shown to influence P-D leaf patterning in monocots
439 like barley and recently, the activity of three, redundant *OsBOP* genes was shown to be
440 required for sheath identity in rice (Tavakol et al., 2015; Toriba et al., 2019). In several
441 monocots, the misexpression of several class I *knox* genes perturb P-D patterning by
442 potentially altering phytohormone ratios in developing leaf primordia (Reiser et al., 2000;
443 Schneeberger et al., 1995; Foster et al., 1999b; Ramirez et al., 2009). Our analysis of
444 *Hsf1*, the second characterized mutation of a maize CK signaling gene, has uncovered

445 a connection between CK and the specification of P-D leaf patterning that is consistent
446 with this hypothesis. How CK drives prong formation is not clear, although the interplay
447 of CK and GA are known to control the degree of leaf complexity in eudicots like
448 *Arabidopsis* and tomato, through the specification of marginal lobes or leaflets (Jasinski
449 et al., 2005; Bar and Ori, 2015). Whether there is any overlap between the
450 mechanism(s) of prong formation in *Hsf1* and leaflet formation in species like tomato will
451 require further analysis. Prong formation itself appears developmentally regulated as
452 prong initiation seems to be coordinated with formation of the ligule suggesting the
453 signals establishing the P-D axis might be transmitted across the entire leaf primordium
454 (Supplemental Figures 1D to 1E). Moreover, prong formation is not random as prongs
455 form only within a certain domain of the blade, with the largest prongs forming more
456 basally (Supplemental Figures 2D to 2F). Intriguingly, this prong-formation region has
457 some overlap with the domain of the leaf blade deleted by mutation of the duplicate
458 *wuschel-related homeobox (wox)* genes *narrow sheath1* and *narrow sheath2*
459 (Nardmann et al., 2004). This implies that the marginal domain specified by these
460 duplicate *wox* transcription factors may provide a permissive context for prongs to form.
461 This hypothesis can be tested by analysis of prong formation in the triple mutant.

462 Leaf sheath and blade length, and blade width were reduced in *Hsf1*
463 heterozygotes compared to wild type sib plants at seedling and mature growth stages,
464 consistent with previous reports, and CK treatment recapitulated this phenotype in wild
465 type inbred seedlings (Figures 2A to 2C) (Bertrand-Garcia and Freeling, 1991b). Since
466 CK activity typically promotes cellular proliferation, how CK hypersignaling reduces
467 growth in the shoot is not known, although increased CK signaling is known to reduce
468 root growth (Werner et al., 2001, 2003). Typically, reducing CK accumulation or
469 signaling results in smaller leaves and other above ground organs, suggesting
470 increased CK activity might be expected to enhance growth (Werner et al., 2001;
471 Nishimura et al., 2004). Growth of the maize leaf is organized linearly along its
472 longitudinal axis into distinct zones of cell division, cell expansion and differentiation
473 (Freeling and Lane, 1992). Recent transcriptome, proteome and hormone profiling
474 studies have enumerated multiple regulatory pathways controlling the size of and

475 transitions between the different growth zones, with GA playing a prominent role (Li et
476 al., 2010; Nelissen et al., 2012; Facette et al., 2013). How increased CK signaling
477 impacts these growth zones to determine final leaf size will require further analysis
478 building upon these previous studies.

479 In addition to a change in P-D patterning and reduction in leaf size, the *Hsf1*
480 mutation and CK treatment of wild type seed promoted increased macrohair formation
481 in the leaf epidermis (Figures 2D to 2E and 2J). Macrohairs are normally found on adult
482 leaves on the abaxial sheath, at high density near the ligule but declining basipetally, on
483 the adaxial blade and along the blade margin. *Hsf1* increased macrohair production not
484 only on the abaxial sheath, adaxial blade, auricle and blade margins of adult leaves but
485 also on juvenile and transitional leaves which are typically glabrous. CK treatment
486 phenocopied the increased pubescence phenotype of *Hsf1* (Figures 2D to 2E). The
487 epidermis of the maize leaf has three types of pubescence – bicellular microhairs,
488 macrohairs and prickly hairs – with macrohairs being the most prominent (Freeling and
489 Lane, 1992). Macrohairs form by differentiation of specialized epidermal cells organized
490 in patterned files beginning in the fifth or sixth leaf (Moose et al., 2004). Little is known
491 regarding the signals specifying macrohair formation, although a recessive mutation
492 affecting macrohair initiation, *macrohairless1*, has been reported (Moose et al., 2004).
493 By contrast, trichome differentiation in the leaves of eudicots, like *Arabidopsis*, is known
494 to be controlled by a core network of positive and negative transcriptional regulators
495 (Ishida et al., 2008; Grebe, 2012; Pattanaik et al., 2014). And trichome initiation on the
496 inflorescence organs in *Arabidopsis* is jointly stimulated by the activity of CK and GA,
497 and downstream transcription factors (Gan et al., 2007; Zhou et al., 2013). The
498 increase in macrohair formation mediated by CK treatment or the *Hsf1* mutant suggests
499 CK can reprogram epidermal cell fate in maize leaves.

500

501 **Missense Mutations in the Maize CK Receptor ZmHK1 underlie the *Hsf1***
502 **phenotype**

503 Our data indicate gain-of-function mutations of the maize CK receptor *ZmHK1* underlie
504 the semi-dominant *Hsf1* mutations. CK signaling, which is well described (To and
505 Kieber, 2008; Hwang et al., 2012), regulates several developmental and physiological
506 processes, although influences on leaf patterning are not among them. For example,
507 combinations of loss of function mutations of the three Arabidopsis CK receptors
508 demonstrate this gene family has partially overlapping and redundant functions in the
509 control of shoot and root growth, seed size, germination and leaf senescence (Higuchi
510 et al., 2004; Nishimura et al., 2004; Riefler et al., 2006). CK receptors were shown to
511 also possess phosphatase activity by analysis of a specific mutation of *AHK4/CRE1*, the
512 recessive *wooden leg (wol)* allele (*CRE1(T278I)*) (Mahonen et al., 2006). Plants
513 homozygous for the *wol* allele have abnormal root vascular development due to the
514 dose-dependent constitutive phosphatase activity of this allele. A gain of function
515 mutation in the CHASE domain of *AHK3 (ore12-1)* revealed this receptor plays a major
516 role in CK-mediated leaf senescence; although how this mutation affected receptor
517 activity was not explored (Kim et al., 2006). The study of gain-of-function mutations has
518 revealed additional information on CK receptor function. Novel, dominant, missense
519 mutations in *AHK2* and *AHK3*, the *repressor of cytokinin deficiency* alleles (*rock2* and
520 *rock3*) enhanced CK signaling, increased CK hypersensitivity, and increased transcript
521 accumulation of CK-responsive genes, similar to the *Hsf1* mutations (Figure 3) (Bartrina
522 et al., 2017). In contrast, the *rock* mutations had the opposite effect on phenotype
523 compared to *Hsf1*, producing early flowering, enlarged rosette leaves and shoots, and
524 longer roots. The contrasting phenotypic effects might be due to differences in signaling
525 strength between the *rock* and *Hsf1* mutations or reflect differences in the downstream
526 circuitry between the two species.

527 **Mutations near the CK binding pocket alter ligand affinity and receptor signaling**

528 To clarify how the function of *ZmHK1* was altered in the *Hsf1* mutants, we
529 analyzed their activity in heterologous his-kinase signaling and ligand binding assays.
530 Our results indicate two of the *Hsf1* mutant receptors signal independent of added CK in
531 yeast and all three have increased binding affinities for the natural CKs tested (Figure
532 1E and Table 1). The mutant receptors may be in a “locked on” state, similar to what

533 was hypothesized for the *snf2* mutation or the increased ligand affinities of the *Hsf1*
534 receptors may explain their ability to signal independent of CK action. We favor the
535 second idea and think the increased CK affinity explains the ability of the mutant
536 receptors to signal in heterologous hosts. Many microbes, including *E. coli* and yeast,
537 contain low concentrations of iP as a normal constituent of tRNA which can become
538 free due to tRNA decay (Skoog and Armstrong, 1970; Hall, 1973; Romanov, 1990; Mok
539 and Mok, 2001). The three mutant receptors all have increased affinity for iP (Table 2).
540 This stronger affinity may be due to stronger complex formation, or longer receptor
541 occupancy and, as a consequence, stronger signaling even in the presence of low iP
542 concentration. Thus, the ability of the ZmHK1-AEWL and ZmHK1-1603 receptors to
543 signal in yeast without added CKs may be due to their increased affinity for iP already
544 present at low concentration in yeast cells (Figure 1E). In fact, it has been shown that
545 expressing other HK receptors in the *sln1* deletion yeast strain TM182 permits this
546 strain to grow on glucose without added CKs, albeit at a much slower rate than with
547 CKs present, and recombinant HKs synthesized in *E. coli* cannot be crystalized without
548 iP complexed in the binding pocket (Higuchi et al., 2009; Hothorn et al., 2011). Since all
549 three mutant receptors have increased ligand affinities (Table 1), have nearly identical
550 mutant plant phenotypes in several different genetic backgrounds (Figure 1 and
551 Supplemental Table 1), and show similar misexpression patterns of CK responsive
552 genes ((Figures 3A) we conclude all three *Hsf1* mutant receptors function similarly *in*
553 *planta*.

554 Our structural analysis localized each residue mutated in *Hsf1* to the ligand-
555 binding Per-Arnt-Sim-like (PAS) subdomain of the CHASE domain in ZmHK1 (Figure
556 1F) (Steklov et al., 2013; Hothorn et al., 2011). Notably, none are within the CK binding
557 pocket or predicted to make contact with the ligand. Rather all are located near a loop
558 domain comprising one face of the pocket suggesting interactions with this loop may
559 affect the binding pocket resulting in increased ligand affinity. Interestingly, amino acid
560 substitutions that rendered *AHK4* constitutively active in a heterologous *E. coli* his-
561 kinase assay were located downstream of the CHASE domain in the second
562 transmembrane domain and near the kinase domain (Miwa et al., 2007). In addition,

563 none of the *rock* mutations are located in the ligand-binding PAS domain (Bartrina et al.,
564 2011). Rather two are in the N-terminal α -helices and one is in the C-terminal
565 transmembrane domain. Therefore, further structure-function studies will be needed to
566 define which residues are crucial for activity and to resolve the precise mechanism(s) by
567 which individual missense mutations alter ligand binding and receptor signaling.

568 ***Hsf1* affects downstream components of CK signaling**

569 More ZmHK1 signaling in developing *Hsf1* leaf primordia resulted in increased
570 transcript accumulation of several early CK response genes in all three *Hsf1* mutant
571 alleles (Figure 3A). Although not all CK reporters responded the same within an allele
572 or tissue, overall our data are consistent with *Hsf1* upregulating CK responsive genes.
573 The most consistent effect was upregulation of *ZmRR3* where its normally meristem-
574 confined expression was expanded in *Hsf1-1603* to include expression near newly
575 arising leaf primordia and in primordia margins (Figure 3B). Notably, the increased CK
576 signaling reported by *ZmRR3* marks the margins of early stage leaf primordia (Figure
577 3B) which is where prongs will form later in development (Supplemental Figures 1F and
578 1G). Although we found ectopic *ZmRR3* signal along the entire margin, outgrowths do
579 not emanate from the entire blade margin but, rather, occur sporadically, with
580 outgrowths interspersed with regions of normal blade margin (Figure 1B and 1C and
581 Supplemental Figure 2A). This observation suggests even though CK hypersignaling
582 can promote proximalization of blade margin cells, not all cells at the margin are
583 competent to respond to this signal. Double mutants heterozygous for *Hsf1-1603* and
584 homozygous for *abph1*, a null allele of *ZmRR3*, show a synergistic interaction (Figure
585 4A and 4B). Several type-A RRs function to negatively regulate CK signal transduction,
586 as well as, regulate circadian rhythms, phytochrome function and meristem size (To et
587 al., 2004). The increased severity of growth defects in *Hsf1* heterozygotes which lack
588 *abph1* activity suggests upregulation of *ZmRR3* (*abph1*) partially ameliorates CK
589 hypersignaling. This also suggests that *ZmRR3* normally functions to attenuate CK
590 signal transduction in maize shoot apices, in addition to specifying leaf phyllotaxy.

591 The identification of the CK receptor *ZmHK1* as the gene underlying the leaf
592 patterning *Hsf1* mutation adds to our understanding of the role CK can play in basic
593 developmental programs. Future studies to determine the molecular determinants
594 functioning downstream of CK signaling that promote prong formation should illuminate
595 mechanisms important for developmental reprogramming and cell fate acquisition.

596 **METHODS**

597 **Plant Material, Genetics, Phenotypic Measurements and Analysis.**

598 The *Hsf1-1595*, *Hsf1-1603* and *Hsf1-2559* mutants arose via EMS mutagenesis
599 of the inbred Mo17 and seed was obtained from the Maize Genetic Cooperation Stock
600 Center (<http://maizecoop.cropsci.uiuc.edu/>). *Hsf1-AEWL* arose via EMS mutagenesis of
601 the inbred A619 and *Hsf1-7322* via EMS mutagenesis of the inbred A632 in
602 independent screens. Homozygous *Hsf1* mutants of all five alleles were identified for
603 sequence analysis from progeny of self-pollinated heterozygous B73 introgressed
604 plants by phenotype and also by PCR screening of linked sequence polymorphisms
605 unique to the progenitor inbred lines and the backcross inbred B73. Since *Hsf1-1595*
606 and *Hsf1-1603* were the same transition mutations as *Hsf1-7322* and *Hsf1-2559*,
607 respectively, further analysis was only performed on three mutants: *Hsf1-1595*, *Hsf1-*
608 *1603* and *Hsf1-AEWL*. All phenotypic, molecular and epistatic analyses were
609 performed on the three alleles that had been backcrossed a minimum of six times to the
610 inbred B73. The *Hsf1* phenotype of the three alleles was fully penetrant as a
611 heterozygote in all backcross generations. Progeny from self- or sib-pollinated *Hsf1*
612 heterozygotes of the three alleles segregated 25% severely stunted, very slow growing,
613 multi-shoot plants that only survived when grown in the greenhouse but were sterile.
614 The *abph1* mutant seed was backcrossed a minimum of three times to the inbred B73
615 before making the double mutant family segregating with *Hsf1-1603*. *Hsf1-1603*
616 heterozygotes were crossed by *abph1* homozygotes and double heterozygous progeny
617 plants were backcrossed by *abph1* homozygotes creating double mutants families
618 segregating 25% +/+, *abph1*/+ (WT); 25% +/+, *abph1/abph1* (single *abph1* mutant);
619 25% *Hsf1*/+, +/*abph1* (single *Hsf1* mutant); and 25% *Hsf1*/+, *abph1/abph1* (double *Hsf1*

620 *abph1* mutant). Allele specific PCR genotyping was done to confirm phenotypes of
621 *Hsf1* heterozygotes and *abph1* heterozygotes and homozygotes (Supplemental Table
622 3).

623 Measurement of adult plant traits of the three *Hsf1* mutant alleles was performed
624 on field grown families segregating 50% wild type: 50% *Hsf1* heterozygotes.
625 Measurements were taken on 7-11 plants of each genotype in 1-row plots with two
626 biological replicates. For analysis of prong position, prong size and percent prong
627 margin, the third leaf above the ear of adult *Hsf1* heterozygous plants was collected
628 from 1-row plots of field grown plants in three replicates in summer 2013.
629 Approximately, 6 to 10 leaves were collected per plot for each allele. For each leaf,
630 measurements were made for (1) total blade length, (2) prong position by measuring the
631 distance from the base of the blade to the mid-point of each prong on each blade
632 margin, and (3) prong size by measuring from the basal to the distal position along the
633 margin where proximal tissue emerged from the blade for each prong (Figure 1B).
634 Percent prong margin was defined as the proportion of leaf blade margin that is
635 occupied by tissue having proximal (sheath, auricle and/or ligule) identity and was
636 calculated by summing the size of all prongs from both sides of the leaf blade divided by
637 twice the length of the leaf blade.

638 Analysis of prong position, prong size and the relationship between prong
639 position and size was estimated with kernel smoothing methods (Silverman, 1986;
640 Wand and Jones, 1995). For all cases a Gaussian kernel was used and the data
641 reflection method was applied for boundary correction since both position and size are
642 positive variables. The bandwidth were selected using least squares cross validation
643 (Bowman, 1984). All computations were performed using R software, kernel density
644 estimation was performed using the *ks* package (Duong, 2007) and figures were
645 created with the *ggplot2* package (Wickham, 2009).

646

647 **Map-based cloning of *Hsf1*.**

648 *Hsf1-1595* was introgressed into B73 and crossed to PRE84 to generate a BC1
649 mapping population. Genetic mapping with 96 BC1 individuals defined *Hsf1* between
650 two SNP markers on chr5: PHA12918-F (204590502 bp, B73 RefGen_v2) and
651 PHA5244-F (206614542 bp, B73 RefGen_v2). The two flanking markers were used to
652 screen a BC1 population of 1500 individuals from B73_*Hsf1* x A632 and 1600 individual
653 from B73_*Hsf1* x PRE84. 224 recombinants were identified, and these individuals were
654 used for further fine mapping. Additional markers derived from the *Hsf1* interval were
655 developed and used to fine map the *Hsf1* mutation with the recombinants, as described
656 in Jiang et al. 2012 (Jiang et al., 2012). The gene underlying the *Hsf1* mutation was
657 finally delimited to a 21 kb interval, between Indel marker 410984 (205538463 bp, B73
658 RefGen_v2, with one recombinant between this marker and *Hsf1*) and SNP marker
659 391087 (205559234 bp, B73 RefGen_v2, with three recombinants between this marker
660 and *Hsf1*). There is only one annotated gene model (B73 RefGen_v3
661 GRMZM2G151223, B73 RefGen_v4 Zm00001d017977) in this interval, that was also
662 annotated in NCBI as LOC541634 histidine kinase1a putative cytokinin receptor.

663

664 **Heterologous histidine kinase assays.** Signaling of the wild type and *Hsf1* mutant
665 ZmHK1 receptors in yeast was performed as described previously (Inoue et al., 2001).
666 The exact point mutations for each of the three *Hsf1* missense mutations were
667 engineered into the cDNA of *ZmHK1* in the plasmid P415-CYC1-ZmHK1 plasmid with
668 the QuikChange II Site-Directed Mutagenesis kit (Agilent Technologies) using the
669 manufacturer's specifications

670

671 **Cytokinin binding affinity determination.** Cytokinin binding assays were performed
672 with recombinant maize cytokinin receptors expressed in *E. coli* cells. Spheroplasts
673 were prepared from cell lines expressing the wild type ZmHK1, and mutant ZmHK1-
674 AEWL and ZmHK1-1603 receptors. Competitive cytokinin binding assays were
675 performed as previously described (Lomin et al., 2011). Transient expression of

676 receptors for the homologous binding assay was done by transformation of tobacco
677 *Nicotiana benthamiana* as previously described (Sparkes et al., 2006). Agrobacteria *A.*
678 *tumefaciens* carrying cytokinin receptor genes fused to GFP were grown in parallel with
679 a helper agrobacterial strain p19 (Voinnet et al., 2003). Five to six week old tobacco
680 plants were infiltrated with the mixture of two agrobacterial strains and the expression
681 level of receptor genes was checked after 4 days using a confocal microscope. For
682 those cases with sufficient expression, leaves were processed further for plant
683 membrane isolation. For plant membrane isolation, all manipulations were done at 4
684 °C. Tobacco leaves were homogenized in buffer containing 300 mM sucrose, 100 mM
685 Tris-HCl (pH 8.0), 10 mM Na₂-EDTA, 0.6% polyvinylpyrrolidone K30, 5 mM K₂S₂O₅, 5
686 mM DTT and 1 mM PMSF. The homogenate was filtered through Miracloth
687 (Calbiochem), and the filtrate was first centrifuged for 10 min at 10000 g, and then for
688 30 min at 100000 g. The microsome pellet was resuspended in PBS (pH 7.4), frozen
689 and stored at -70 °C before using.

690

691 **ZmHK1 structure modeling.**

692 The amino acid sequence of the ZmHK1 CHASE domain (86-270) was obtained from
693 the protein sequence database of NCBI (accession id: NP_001104859). It shares 71%
694 sequence identity with the *Arabidopsis HK4* sensor domain. The homology model for
695 ZmHK1 was generated using Swiss model server (<http://swissmodel.expasy.org>) with
696 the published crystal structure of AHK4 (pdb code: 3T4J) as a template. Subsequently
697 the model was solvated and subjected to energy minimization using the steepest
698 descent followed by conjugate gradient algorithm to remove clashes. The
699 stereochemical quality of the ZmHK1 model was assessed using the PROCHECK
700 program. None of the residues were in the disallowed regions of the Ramachandran
701 map.

702 **Exogenous CK treatment.**

703 Exogenous CK treatments were performed with 6-benzylaminopurine (6-BAP) (Sigma
704 Aldrich) dissolved in 10 drops 1N NaOH and brought to 1mM concentration with distilled
705 water. All water control treatments were done using a similar stock of 10 drops 1N
706 NaOH and diluted in parallel to the CK stock. Further dilutions to the desired CK
707 concentration were done with distilled water. Maize kernels were surface sterilized with
708 two 5 minute washes of 80% ethanol followed by two 15 minute washes of 50% bleach
709 and rinsed five times in sterile distilled water. Kernels were imbibed overnight with
710 sterile distilled water prior to the start of the hormone treatment. For hormone
711 treatments, 20 imbibed kernels per replicate were placed embryo-side down on two
712 paper towels in a petri dish, covered with two more layers of paper towel and filled with
713 15 mL of CK treatment or the water control solution. Petri dishes were sealed with
714 parafilm and placed in a lab drawer in the dark at room temperature for 6 days. After
715 treatment, germinating kernels were rinsed with sterile, distilled water and planted in 4
716 cm square pots in soilless potting medium (Metro-Mix 900, SunGro Horticulture) and
717 grown in the greenhouse (day: 16 hr./28°C, night: 8 hr./21°C) with supplemental lighting
718 (high pressure sodium and metal halide lights) and standard light intensity ($230 \mu\text{E m}^{-2}$
719 s^{-1} at height of 3.5 feet). Growth was monitored and leaf measurements were taken
720 after the fourth leaf collar (auricle and ligule) had fully emerged from the whorl after 3-4
721 weeks. For measurements, individual leaves were removed from the plant and each
722 component measured. Leaf sheath length was defined as the site of insertion of the
723 leaf base to the culm (stem) to the farthest point of sheath adjoining the ligule. Leaf
724 blade length was defined as the most proximal point of blade adjoining the ligule to the
725 distal blade tip. Leaf blade width was measured margin to margin at half of the leaf
726 blade length. All leaf measurements were analyzed using JMP PRO 12 software using
727 a student's t-test to determine significance with two comparisons, and Tukey's HSD test
728 to determine significance with more than two comparisons. To examine macrohair
729 abundance, epidermal impressions were made using Crazy Glue Maximum Bond®
730 cyanoacrylate glue applied to a Fisherbrand Superfrost Plus® microscope slide. The
731 adaxial blade of leaf one was pressed firmly into the glue for about 30 seconds, followed
732 by immediate removal of the leaf. Slides were imaged on an Olympus BX60 light
733 microscope.

734

735 **Expression analysis.**

736 ***In situ* hybridization:**

737 For *in situ* hybridization, we slightly modified an online protocol from Jeff Long. For
738 complete details refer to http://pbio.salk.edu/pbiol/in_situ_protocol.html. *In situ* probes
739 were made using T7/SP6 promoter based *in vitro* transcription in the cloning vector
740 pGEMT (Promega). FAA (Formaldehyde Acetic Acid) fixed and paraffin embedded
741 maize shoot apices were sectioned at 10 μ thickness and laid on Probe-On-Plus slides
742 (Fisher) and placed on a warmer at 42°C. After overnight incubation the slides were
743 deparaffinized using Histo- Clear (National Diagnostics), treated with proteinase K and
744 dehydrated. Probes were applied on the slides and pairs of slides were sandwiched
745 carefully and incubated at 55°C overnight. The following day the slides were rinsed and
746 washed. Diluted (1:1250) anti-DIG-antibody (Roche) was applied to the slides and
747 incubated for 2 hours. After thoroughly washing the slides, sandwiched slides were
748 placed in NBT-BCIP (Roche) solution (200 μ l in 10ml buffer C; 100mM Tris
749 pH9.5/100mM NaCl/50mM MgCl₂) in dark for 2-3 days for color development. Color
750 development reaction was stopped using 1x Tris EDTA. The slides were mounted using
751 Immu-Mount (Thermo Scientific) and observed and imaged under a bright field
752 microscope.

753

754 **RT qPCR:**

755 Seedling tissue was collected from two-week old, stage V3 – V4 *Hsf1*^{+/+} and wild type
756 sib seedlings for each allele and included (1) ca. 2 cm of mature green leaf blade from
757 the distal half of leaf #4, (2) ca. a 2 cm cylinder of immature leaf tissue, cut ca. 1 cm
758 above the insertion point of leaf #5 after removing leaf #4, and (3) the remaining 1 cm
759 cylinder of tissue above the insertion point of leaf #5, consisting of the SAM, young leaf
760 primordia and the apical part of the stem. Tissue was bulked from three different plants

761 for each biological replicate and three replicates were collected. Total RNA was
762 extracted from these tissues using Trizol reagent, adhering to the manufacturer's
763 protocol (http://tools.lifetechnologies.com/content/sfs/manuals/trizol_reagent.pdf).
764 cDNA was synthesized from total RNA using the SuperScript® III First-Strand
765 (Invitrogen) synthesis system for reverse transcriptase PCR (RT-CPR) and oligo-d(T)
766 primers. Quantitative real-time PCR was performed on the cDNA using an LC480
767 (Roche) and the SYBR green assay. The primers were designed near the 3' end of the
768 gene with an amplicon size of between 120 bp to 250 bp Folylpolylglutamate synthase
769 (FPGS) was used as an endogenous control as it was shown to have very stable
770 expression across a variety of maize tissues and range of experimental conditions
771 (Manoli et al., 2012). Two technical replicates were included for each gene.
772 Comparative $\Delta\Delta\text{Ct}$ method was used to calculate fold change compared to the
773 endogenous control. ΔCt of mutant (*Hsf1*) and ΔCt of wild type (WT) was expressed as
774 the difference in Ct value between target gene and the endogenous control. $\Delta\Delta\text{Ct}$ was
775 then calculated as the difference of ΔCt (*Hsf1*) and ΔCt (WT). Finally, fold change in
776 target gene expression between *Hsf1* and WT was determined as $2^{-\Delta\Delta\text{Ct}}$.

777

778 **Acknowledgements**

779 We thank Dave Jackson (Cold Spring Harbor Labs) for the *abph1* mutant seed, Erica
780 Unger-Wallace (Iowa State University) for technical assistance and Erik Vollbrecht
781 (Iowa State University) for support during the early phase of this research. D.M.K.,
782 S.N.L. and G.A.R. were partly supported by the Molecular and Cell Biology Program of
783 the Presidium of RAS. . This work was supported by the National Science Foundation
784 under Grant Number 1022452.

785

786 **Author contributions**

787 M.G.M., S.C., H.S., G.A.R., B.L. and N.B. designed research; L.M.T., S.C., J.C.,
788 A.D.V.E., I.A., A.P., D.M.K., S.N.L., S.T., T.D., and N. M. performed research; M.G.M.,
789 H.S., G.A.R., B.L. and N.B. analyzed data; and M.G.M. wrote the paper with input from
790 the other authors.

791

792

793

794 **REFERENCES**

- 795 **Asakura, Y., Hagino, T., Ohta, Y., Aoki, K., Yonekura-Sakakibara, K., Deji, A.,**
796 **Yamaya, T., Sugiyama, T., and Sakakibara, H.** (2003). Molecular characterization
797 of His-Asp phosphorelay signaling factors in maize leaves: Implications of the
798 signal divergence by cytokinin-inducible response regulators in the cytosol and the
799 nuclei. *Plant Mol. Biol.* **52**: 331–341.
- 800 **Bar, M. and Ori, N.** (2015). Compound leaf development in model plant species. *Curr.*
801 *Opin. Plant Biol.* **23**: 61–69.
- 802 **Bartrina, I., Jensen, H., Novák, O. rej, Strnad, M., Werner, T., and Schmölling, T.**
803 (2017). Gain-of-Function Mutants of the Cytokinin Receptors AHK2 and AHK3
804 Regulate Plant Organ Size, Flowering Time and Plant Longevity. *Plant Physiol.*
805 **173**: 1783–1797.
- 806 **Bartrina, I., Otto, E., Strnad, M., Werner, T., and Schmölling, T.** (2011). Cytokinin
807 Regulates the Activity of Reproductive Meristems, Flower Organ Size, Ovule
808 Formation, and Thus Seed Yield in *Arabidopsis thaliana*. *Plant Cell Online* **23**: 69–
809 80.
- 810 **Benjamins, R. and Scheres, B.** (2008). Auxin: The Looping Star in Plant Development.
811 *Annu. Rev. Plant Biol.* **59**: 443–465.
- 812 **Bertrand-Garcia, R. and Freeling, M.** (1991a). Hairy-Sheath Frayed #1-O: A Systemic,
813 Heterochronic Mutant of Maize That Specifies Slow Developmental Stage
814 Transitions. *Am. J. Bot.* **78**: 747–765.
- 815 **Bertrand-Garcia, R. and Freeling, M.** (1991b). Hsf1-O (Hairy sheath frayed): 5L
816 linkage data. *Maize Genet. Coop. News Lett.*: 30.
- 817 **Bird, R.M. and Neuffer, M.G.** (1985). Developmentally Interesting New Mutants in
818 Plants Odd New Dominant Mutations Affecting the Development of the Maize Leaf.
819 Free. M. (Ed.). Ucla (University Calif. Los Angeles) Symp. Mol. Cell. Biol. New Ser.
820 Vol. 35. Plant Genet. Third Annu. Arco Plant Cell Res. Institute-Ucla Symp. Plant

- 821 Biol. Keystone, Colo., USA, Apr. 13-: 818–822.
- 822 **Bolduc, N. and Hake, S.** (2009). The Maize Transcription Factor KNOTTED1 Directly
823 Regulates the Gibberellin Catabolism Gene *ga2ox1*. *Plant Cell* **21**: 1647–1658.
- 824 **Bowman, A.W.** (1984). An alternative method of cross-validation for the smoothing of
825 density estimates. *Biometrika* **71**: 353–360.
- 826 **Bowman, J.L., Eshed, Y., and Baum, S.F.** (2002). Establishment of polarity in
827 angiosperm lateral organs. *Trends Genet.* **18**: 134–141.
- 828 **Byrne, M., Timmermans, M., Kidner, C., and Martienssen, R.** (2001). Development of
829 leaf shape. *Curr. Opin. Plant Biol.* **4**: 38–43.
- 830 **Byrne, M.E., Simorowski, J., and Martienssen, R.A.** (2002). ASYMMETRIC
831 LEAVES1 reveals *knox* gene redundancy in Arabidopsis. *Development* **129**: 1957–
832 1965.
- 833 **Du, L., Jiao, F., Chu, J., Jin, G., Chen, M., and Wu, P.** (2007). The two-component
834 signal system in rice (*Oryza sativa* L.): A genome-wide study of cytokinin signal
835 perception and transduction. *Genomics* **89**: 697–707.
- 836 **Duong, T.** (2007). ks: Kernel density estimation and kernel discriminant analysis for
837 multivariate data in R. *J. Stat. Softw.* **21**: 1–16.
- 838 **Edgar, R.C.** (2004). MUSCLE: multiple sequence alignment with high accuracy and
839 high throughput. *Nucleic Acids Res.* **32**: 1792–1797.
- 840 **Endrizzi, K., Moussian, B., Haecker, A., Levin, J.Z., and Laux, T.** (1996). The
841 SHOOT MERISTEMLESS gene is required for maintenance of undifferentiated
842 cells in Arabidopsis shoot and floral meristems and acts at a different regulatory
843 level than the meristem genes *WUSCHEL* and *ZWILLE*. *Plant J.* **10**: 967–979.
- 844 **Facette, M.R., Shen, Z., Björnsdóttir, F.R., Briggs, S.P., and Smith, L.G.** (2013).
845 Parallel Proteomic and Phosphoproteomic Analyses of Successive Stages of Maize
846 Leaf Development. *Plant Cell* **25**: 2798–2812.
- 847 **Foster, T., Veit, B., and Hake, S.** (1999a). Mosaic analysis of the dominant mutant,
848 *Gnarley1-R*, reveals distinct lateral and transverse signaling pathways during maize

- 849 leaf development. *Development* **126**: 305–313.
- 850 **Foster, T., Yamaguchi, J., Wong, B.C., Veit, B., and Hake, S.** (1999b). Gnarley1 Is a
851 Dominant Mutation in the *knox4* Homeobox Gene Affecting Cell Shape and Identity.
852 *Plant Cell* **11**: 1239–1252.
- 853 **Freeling, M. and Hake, S.** (1985). Developmental genetics of mutants that specify
854 Knotted leaves in maize. *Genetics* **111**: 617–634.
- 855 **Freeling, M. and Lane, B.** (1992). The maize leaf. In *The Maize Handbook*, M. Freeling
856 and V. Walbot, eds (Springer-Verlag: New York LB - PBS Record: 390), p. in
857 press.
- 858 **Gan, Y., Liu, C., Yu, H., and Broun, P.** (2007). Integration of cytokinin and gibberellin
859 signalling by Arabidopsis transcription factors GIS, ZFP8 and GIS2 in the regulation
860 of epidermal cell fate. *Development* **134**: 2073–2081.
- 861 **Giulini, A., Wang, J., and Jackson, D.** (2004). Control of phyllotaxy by the cytokinin-
862 inducible response regulator homologue ABPHYL1. *Nature* **430**: 1031–1034.
- 863 **van der Graaff, E., Dulk-Ras, A.D., Hooykaas, P.J., and Keller, B.** (2000). Activation
864 tagging of the *LEAFY PETIOLE* gene affects leaf petiole development in
865 *Arabidopsis thaliana*. *Development* **127**: 4971–4980.
- 866 **van der Graaff, E., Nussbaumer, C., and Keller, B.** (2003). The *Arabidopsis thaliana*
867 *rlp* mutations revert the ectopic leaf blade formation conferred by activation tagging
868 of the *LEP* gene. *Mol. Genet. Genomics* **270**: 243–252.
- 869 **Grebe, M.** (2012). The patterning of epidermal hairs in *Arabidopsis* — updated. *Curr.*
870 *Opin. Plant Biol.* **15**: 31–37.
- 871 **Guo, M., Thomas, J., Collins, G., and Timmermans, M.C.P.** (2008). Direct
872 Repression of *KNOX* Loci by the *ASYMMETRIC LEAVES1* Complex of
873 *Arabidopsis*. *Plant Cell* **20**: 48–58.
- 874 **Ha, C.M., Jun, J.H., Nam, H.G., and Fletcher, J.C.** (2004). *BLADE-ON-PETIOLE1*
875 encodes a BTB/POZ domain protein required for leaf morphogenesis in
876 *Arabidopsis thaliana*. *Plant Cell Physiol* **45**: 1361–1370.

- 877 **Ha, C.M., Kim, G.T., Kim, B.C., Jun, J.H., Soh, M.S., Ueno, Y., Machida, Y.,**
878 **Tsukaya, H., and Nam, H.G.** (2003). The BLADE-ON-PETIOLE 1 gene controls
879 leaf pattern formation through the modulation of meristematic activity in
880 Arabidopsis. *Development* **130**: 161–172.
- 881 **Hake, S., Sinha, N., Veit, B., Vollbrecht, E., and Walko, R.** (1991). Mutations of
882 Knotted alter cell interactions in the developing maize leaf. In *Plant Molecular*
883 *Biology*, R.G. Herrmann and B. Larkins, eds (Plenum Press: New York), pp. 555–
884 562.
- 885 **Hake, S., Vollbrecht, E., and Freeling, M.** (1989). Cloning Knotted, the dominant
886 morphological mutant in maize using Ds2 as a transposon tag. *EMBO J.* **8**: 15–22.
- 887 **Hall, R.H.** (1973). Cytokinins as a probe of developmental processes. *Annu. Rev.*
888 *Plant Physiol.* **24**: 415–444.
- 889 **Hay, A., Barkoulas, M., and Tsiantis, M.** (2006). ASYMMETRIC LEAVES1 and auxin
890 activities converge to repress BREVIPEDICELLUS expression and promote leaf
891 development in Arabidopsis. *Development* **133**: 3955–3961.
- 892 **Hay, A., Kaur, H., Phillips, A., Hedden, P., Hake, S., and Tsiantis, M.** (2002). The
893 gibberellin pathway mediates KNOTTED1-type homeobox function in plants with
894 different body plans. *Curr Biol* **12**: 1557–1565.
- 895 **Higuchi, M. et al.** (2004). In planta functions of the Arabidopsis cytokinin receptor
896 family. *PNAS* **101**: 8821–8826.
- 897 **Higuchi, M., Kakimoto, T., and Mizuno, T.** (2009). *Cytokinin Sensing Systems Using*
898 *Microorganisms Plant Hormones* S. Cutler and D. Bonetta, eds (Humana Press).
- 899 **Hothorn, M., Dabi, T., and Chory, J.** (2011). Structural basis for cytokinin recognition
900 by Arabidopsis thaliana histidine kinase 4. *Nat Chem Biol* **7**: 766–768.
- 901 **Hwang, I. and Sakakibara, H.** (2006). Cytokinin biosynthesis and perception. *Physiol.*
902 *Plant.* **126**: 528–538.
- 903 **Hwang, I. and Sheen, J.** (2001). Two-component circuitry in Arabidopsis cytokinin
904 signal transduction. *Nature* **413**: 383–389.

- 905 **Hwang, I., Sheen, J., and Müller, B.** (2012). Cytokinin Signaling Networks. *Annu. Rev.*
906 *Plant Biol.* **63**: 353–380.
- 907 **Inoue, T., Higuchi, M., Hashimoto, Y., Seki, M., Kobayashi, M., Kato, T., Tabata, S.,**
908 **Shinozaki, K., and Kakimoto, T.** (2001). Identification of CRE1 as a cytokinin
909 receptor from Arabidopsis. *Nature* **409**: 1060–1063.
- 910 **Ishida, T., Kurata, T., Okada, K., and Wada, T.** (2008). A Genetic Regulatory Network
911 in the Development of Trichomes and Root Hairs. *Annu. Rev. Plant Biol.* **59**: 365–
912 386.
- 913 **Jackson, D. and Hake, S.** (1999). Control of phyllotaxy in maize by the *abphyl1* gene.
914 *Development* **126**: 315–323.
- 915 **Jasinski, S., Piazza, P., Craft, J., Hay, A., Woolley, L., Rieu, I., Phillips, A., Hedden,**
916 **P., and Tsiantis, M.** (2005). KNOX action in Arabidopsis is mediated by coordinate
917 regulation of cytokinin and gibberellin activities. *Curr Biol* **15**: 1560–1565.
- 918 **Jiang, F., Guo, M., Yang, F., Duncan, K., Jackson, D., Rafalski, A., Wang, S., and**
919 **Li, B.** (2012). Mutations in an AP2 Transcription Factor-Like Gene Affect Internode
920 Length and Leaf Shape in Maize. *PLoS One* **7**: e37040.
- 921 **Johnston, R., Wang, M., Sun, Q., Sylvester, A.W., Hake, S., and Scanlon, M.J.**
922 (2014). Transcriptomic Analyses Indicate That Maize Ligule Development
923 Recapitulates Gene Expression Patterns That Occur during Lateral Organ Initiation.
924 *Plant Cell* **26**: 4718–4732.
- 925 **Kerstetter, R., Vollbrecht, E., Lowe, B., Veit, B., Yamaguchi, J., and Hake, S.**
926 (1994). Sequence analysis and expression patterns divide the maize knotted1-like
927 homeobox genes into two classes. *Plant Cell* **6**: 1877–1887.
- 928 **Kerstetter, R.A. and Poethig, R.S.** (1998). The specification of leaf identity during
929 shoot development. *Annu. Rev. Cell Dev. Biol.* **14**: 373–398.
- 930 **Kim, H.J., Ryu, H., Hong, S.H., Woo, H.R., Lim, P.O., Lee, I.C., Sheen, J., Nam,**
931 **H.G., and Hwang, I.** (2006). Cytokinin-mediated control of leaf longevity by AHK3
932 through phosphorylation of ARR2 in Arabidopsis. *PNAS* **103**: 814–819.
- 933 **Li, P. et al.** (2010). The developmental dynamics of the maize leaf transcriptome. *Nat.*

- 934 Genet. **42**: 1060–1067.
- 935 **Lomin, S.N., Krivosheev, D.M., Steklov, M.Y., Arkhipov, D.V., Osolodkin, D.I.,**
936 **Schmülling, T., and Romanov, G.A.** (2015). Plant membrane assays with
937 cytokinin receptors underpin the unique role of free cytokinin bases as biologically
938 active ligands. *J. Exp. Bot.* **66**: 1851–1863.
- 939 **Lomin, S.N., Yonekura-Sakakibara, K., Romanov, G.A., and Sakakibara, H.** (2011).
940 Ligand-binding properties and subcellular localization of maize cytokinin receptors.
941 *J. Exp. Bot.* **62**: 5149–5159.
- 942 **Long, J.A., Moan, E.I., Medford, J.I., and Barton, M.K.** (1996). A member of the
943 KNOTTED class of homeodomain proteins encoded by the STM gene of
944 *Arabidopsis*. *Nature* **379**: 66–69.
- 945 **Mahonen, A.P., Higuchi, M., Tormakangas, K., Miyawaki, K., Pischke, M.S.,**
946 **Sussman, M.R., Helariutta, Y., and Kakimoto, T.** (2006). Cytokinins Regulate a
947 Bidirectional Phosphorelay Network in *Arabidopsis*. *Curr. Biol.* **16**: 1116–1122.
- 948 **Manoli, A., Sturaro, A., Trevisan, S., Quaggiotti, S., and Nonis, A.** (2012). Evaluation
949 of candidate reference genes for qPCR in maize. *J. Plant Physiol.* **169**: 807–815.
- 950 **McConnell, J.R. and Barton, M.K.** (1998). Leaf polarity and meristem formation in
951 *Arabidopsis*. *Development* **125**: 2935–2942.
- 952 **Miwa, K., Ishikawa, K., Terada, K., Yamada, H., Suzuki, T., Yamashino, T., and**
953 **Mizuno, T.** (2007). Identification of Amino Acid Substitutions that Render the
954 *Arabidopsis* Cytokinin Receptor Histidine Kinase AHK4 Constitutively Active. *Plant*
955 *Cell Physiol* **48**: 1809–1814.
- 956 **Mok, D.W. and Mok, M.C.** (2001). CYTOKININ METABOLISM AND ACTION. *Annu.*
957 *Rev. Plant Physiol. Plant Mol. Biol.* **52**: 89–118.
- 958 **Moon, J., Candela, H., and Hake, S.** (2013). The Liguleless narrow mutation affects
959 proximal-distal signaling and leaf growth. *Development* **140**: 405–412.
- 960 **Moose, S.P., Lauter, N., and Carlson, S.R.** (2004). The Maize macrohairless1 Locus
961 Specifically Promotes Leaf Blade Macrohair Initiation and Responds to Factors
962 Regulating Leaf Identity. *Genetics* **166**: 1451–1461.

- 963 **Muehlbauer, G.J., Fowler, J.E., and Freeling, M.** (1997). Sectors expressing the
964 homeobox gene *liguleless3* implicate a time-dependent mechanism for cell fate
965 acquisition along the proximal-distal axis of the maize leaf. *Development* **124**:
966 5097–5106.
- 967 **Muller, B. and Sheen, J.** (2008). Cytokinin and auxin interaction in root stem-cell
968 specification during early embryogenesis. *Nature* **453**: 1094–1097.
- 969 **Nardmann, J., Ji, J., Werr, W., and Scanlon, M.J.** (2004). The maize duplicate genes
970 *narrow sheath1* and *narrow sheath2* encode a conserved homeobox gene function
971 in a lateral domain of shoot apical meristems. *Development* **131**: 2827–2839.
- 972 **Nelissen, H., Rymer, B., Jikumaru, Y., Demuyne, K., Van Lijsebettens, M.,
973 Kamiya, Y., Inzé, D., and Beemster, G.T.S.** (2012). A Local Maximum in
974 Gibberellin Levels Regulates Maize Leaf Growth by Spatial Control of Cell Division.
975 *Curr. Biol.* **22**: 1183–1187.
- 976 **Nishimura, C., Ohashi, Y., Sato, S., Kato, T., Tabata, S., and Ueguchi, C.** (2004).
977 Histidine Kinase Homologs That Act as Cytokinin Receptors Possess Overlapping
978 Functions in the Regulation of Shoot and Root Growth in Arabidopsis. *Plant Cell*
979 **16**: 1365–1377.
- 980 **Norberg, M., Holmlund, M., and Nilsson, O.** (2005). The *BLADE ON PETIOLE* genes
981 act redundantly to control the growth and development of lateral organs.
982 *Development* **132**: 2203–2213.
- 983 **Ohno, C.K., Reddy, G.V., Heisler, M.G.B., and Meyerowitz, E.M.** (2004). The
984 Arabidopsis *JAGGED* gene encodes a zinc finger protein that promotes leaf tissue
985 development. *Development* **131**: 1111–1122.
- 986 **Ori, N., Eshed, Y., Chuck, G., Bowman, J.L., and Hake, S.** (2000). Mechanisms that
987 control *knox* gene expression in the Arabidopsis shoot. *Development* **127**: 5523–
988 5532.
- 989 **Pattanaik, S., Patra, B., Singh, S., and Yuan, L.** An overview of the gene regulatory
990 network controlling trichome development in the model plant, Arabidopsis. *Front.*
991 *Plant Sci.* **5**: 259.

- 992 **Pozzi, C., Rossini, L., and Agosti, F.** (2001). Patterns and symmetries in leaf
993 development. *Semin Cell Dev Biol* **12**: 363–372.
- 994 **Ramirez, J., Bolduc, N., Lisch, D., and Hake, S.** (2009). Distal Expression of knotted1
995 in Maize Leaves Leads to Reestablishment of Proximal/Distal Patterning and Leaf
996 Dissection. *Plant Physiol.* **151**: 1878–1888.
- 997 **Rashotte, A.M., Mason, M.G., Hutchison, C.E., Ferreira, F.J., Schaller, G.E., and**
998 **Kieber, J.J.** (2006). A subset of Arabidopsis AP2 transcription factors mediates
999 cytokinin responses in concert with a two-component pathway. *PNAS* **103**: 11081–
1000 11085.
- 1001 **Reiser, L., Sanchez-Baracaldo, P., and Hake, S.** (2000). Knots in the family tree:
1002 evolutionary relationships and functions of knox homeobox genes. *Plant Mol Biol*
1003 **42**: 151–166.
- 1004 **Riefler, M., Novak, O., Strnad, M., and Schmulling, T.** (2006). Arabidopsis Cytokinin
1005 Receptor Mutants Reveal Functions in Shoot Growth, Leaf Senescence, Seed
1006 Size, Germination, Root Development, and Cytokinin Metabolism. *Plant Cell* **18**:
1007 40–54.
- 1008 **Romanov, G.A.** (1990). Cytokinins and tRNAs: a hypothesis on their competitive
1009 interaction via specific receptor proteins. *Plant. Cell Environ.* **13**: 751–754.
- 1010 **Romanov, G.A., Spíchal, L., Lomin, S.N., Strnad, M., and Schmülling, T.** (2005). A
1011 live cell hormone-binding assay on transgenic bacteria expressing a eukaryotic
1012 receptor protein. *Anal. Biochem.* **347**: 129–134.
- 1013 **Ronquist, F. and Huelsenbeck, J.P.** (2003). MrBayes 3: Bayesian phylogenetic
1014 inference under mixed models. *Bioinformatics* **19**: 1572–1574.
- 1015 **Sakamoto, T., Kamiya, N., Ueguchi-Tanaka, M., Iwahori, S., and Matsuoka, M.**
1016 (2001). KNOX homeodomain protein directly suppresses the expression of a
1017 gibberellin biosynthetic gene in the tobacco shoot apical meristem. *Genes Dev* **15**:
1018 581–590.
- 1019 **Sakamoto, T., Sakakibara, H., Kojima, M., Yamamoto, Y., Nagasaki, H., Inukai, Y.,**
1020 **Sato, Y., and Matsuoka, M.** (2006). Ectopic Expression of KNOTTED1-Like

- 1021 Homeobox Protein Induces Expression of Cytokinin Biosynthesis Genes in Rice.
1022 *Plant Physiol.* **142**: 54–62.
- 1023 **Scarpella, E., Marcos, D., Friml, J., and Berleth, T.** (2006). Control of leaf vascular
1024 patterning by polar auxin transport. *Genes Dev.* **20**: 1015–1027.
- 1025 **Schneeberger, R.G., Becraft, P.W., Hake, S., and Freeling, M.** (1995). Ectopic
1026 expression of the knox homeo box gene rough sheath1 alters cell fate in the maize
1027 leaf. *Genes Dev.* **9**: 2292–2304.
- 1028 **Shani, E., Yanai, O., and Ori, N.** (2006). The role of hormones in shoot apical meristem
1029 function. *Curr. Opin. Plant Biol.* **9**: 484–489.
- 1030 **Silverman, B.W.** (1986). Density estimation for statistics and data analysis (Chapman
1031 and Hall).
- 1032 **Skoog, F. and Armstrong, D.** (1970). Cytokinins. *Annu. Rev. Plant Physiol.* **21**: 359–
1033 384.
- 1034 **Smith, L.G., Greene, B., Veit, B., and Hake, S.L.B.-P.B.S.R. 3380** (1992). A dominant
1035 mutation in the maize homeobox gene, Knotted-1, causes its ectopic expression in
1036 leaf cells with altered fates. *Development* **116**: 21–30.
- 1037 **Sparkes, I.A., Runions, J., Kearns, A., and Hawes, C.** (2006). Rapid, transient
1038 expression of fluorescent fusion proteins in tobacco plants and generation of stably
1039 transformed plants. *Nat. Protoc.* **1**: 2019–2025.
- 1040 **Steklov, M., Lomin, S.N., Osolodkin, D.I., and Romanov, G.A.** (2013). Structural
1041 basis for cytokinin receptor signaling: an evolutionary approach. *Plant Cell Rep.* **32**:
1042 781–793.
- 1043 **Suzuki, T., Ishikawa, K., Yamashino, T., and Mizuno, T.** (2002). An Arabidopsis
1044 Histidine-Containing Phosphotransfer (HPt) Factor Implicated in Phosphorelay
1045 Signal Transduction: Overexpression of AHP2 in Plants Results in
1046 Hypersensitiveness to Cytokinin. *Plant Cell Physiol* **43**: 123–129.
- 1047 **Suzuki, T., Miwa, K., Ishikawa, K., Yamada, H., Aiba, H., and Mizuno, T.** (2001). The
1048 Arabidopsis Sensor His-kinase, AHK4, Can Respond to Cytokinins. *Plant Cell*
1049 *Physiol.* **42**: 107–113.

- 1050 **Sylvester, A.W., Cande, W.Z., and Freeling, M.** (1990). Division and differentiation
1051 during normal and liguleless-1 maize leaf development. *Development* **110**: 985–
1052 1000.
- 1053 **Sylvester, A.W., Smith, L., and Freeling, M.** (1996). Acquisition of identity in the
1054 developing leaf. *Annu. Rev. Cell Dev. Biol.* **12**: 257–304.
- 1055 **Tavakol, E. et al.** (2015). The Barley Uniculme4 Gene Encodes a BLADE-ON-
1056 PETIOLE-Like Protein That Controls Tillering and Leaf Patterning. *Plant Physiol.*
1057 **168**: 164 LP – 174.
- 1058 **Tirichine, L., Sandal, N., Madsen, L.H., Radutoiu, S., Albrechtsen, A.S., Sato, S.,**
1059 **Asamizu, E., Tabata, S., and Stougaard, J.** (2007). A Gain-of-Function Mutation
1060 in a Cytokinin Receptor Triggers Spontaneous Root Nodule Organogenesis.
1061 *Science* (80-.). **315**: 104–107.
- 1062 **To, J.P.C., Haberer, G., Ferreira, F.J., Deruere, J., Mason, M.G., Schaller, G.E.,**
1063 **Alonso, J.M., Ecker, J.R., and Kieber, J.J.** (2004). Type-A Arabidopsis Response
1064 Regulators Are Partially Redundant Negative Regulators of Cytokinin Signaling.
1065 *Plant Cell* **16**: 658–671.
- 1066 **To, J.P.C. and Kieber, J.J.** (2008). Cytokinin signaling: two-components and more.
1067 *Trends Plant Sci.* **13**: 85–92.
- 1068 **Toriba, T., Tokunaga, H., Shiga, T., Nie, F., Naramoto, S., Honda, E., Tanaka, K.,**
1069 **Taji, T., Itoh, J.-I., and Kyojuka, J.** (2019). BLADE-ON-PETIOLE genes
1070 temporally and developmentally regulate the sheath to blade ratio of rice leaves.
1071 *Nat. Commun.* **10**: 619.
- 1072 **Tsiantis, M., Schneeberger, R., Golz, J.F., Freeling, M., and Langdale, J.A.** (1999).
1073 The maize rough sheath2 gene and leaf development programs in monocot and
1074 dicot plants. *Science* (80-.). **284**: 154–156.
- 1075 **Tsuda, K., Kurata, N., Ohyanagi, H., and Hake, S.** (2014). Genome-Wide Study of
1076 KNOX Regulatory Network Reveals Brassinosteroid Catabolic Genes Important for
1077 Shoot Meristem Function in Rice. *Plant Cell* **26**: 3488–3500.
- 1078 **Tsukaya, H.** (1998). Genetic evidence for polarities that regulate leaf morphogenesis. *J.*

- 1079 Plant Res. **111**: 113–119.
- 1080 **Voinnet, O., Rivas, S., Mestre, P., and Baulcombe, D.** (2003). An enhanced transient
1081 expression system in plants based on suppression of gene silencing by the p19
1082 protein of tomato bushy stunt virus. *Plant J.* **33**: 949–956.
- 1083 **Wand, M.P. and Jones, M.C.** (1995). *Kernel Smoothing Vol. 60 of Monographs on*
1084 *statistics and applied probability.* (Chapman and Hall, London).
- 1085 **Werner, T., Motyka, V., Laucou, V., Smets, R., Van Onckelen, H., and Schmölling,**
1086 **T.** (2003). Cytokinin-Deficient Transgenic Arabidopsis Plants Show Multiple
1087 Developmental Alterations Indicating Opposite Functions of Cytokinins in the
1088 Regulation of Shoot and Root Meristem Activity. *Plant Cell* **15**: 2532–2550.
- 1089 **Werner, T., Motyka, V., Strnad, M., and Schmölling, T.** (2001). Regulation of plant
1090 growth by cytokinin. *PNAS* **98**: 10487–10492.
- 1091 **Wickham, H.** (2009). *ggplot2* (Springer New York: New York).
- 1092 **Yamada, H., Suzuki, T., Terada, K., Takei, K., Ishikawa, K., Miwa, K., Yamashino,**
1093 **T., and Mizuno, T.** (2001). The Arabidopsis AHK4 Histidine Kinase is a Cytokinin-
1094 Binding Receptor that Transduces Cytokinin Signals Across the Membrane. *Plant*
1095 *Cell Physiol* **42**: 1017–1023.
- 1096 **Yanai, O., Shani, E., Dolezal, K., Tarkowski, P., Sablowski, R., Sandberg, G.,**
1097 **Samach, A., and Ori, N.** (2005). Arabidopsis KNOXI Proteins Activate Cytokinin
1098 Biosynthesis. *Curr. Biol.* **15**: 1566–1571.
- 1099 **Yonekura-Sakakibara, K., Kojima, M., Yamaya, T., and Sakakibara, H.** (2004).
1100 Molecular Characterization of Cytokinin-Responsive Histidine Kinases in Maize.
1101 Differential Ligand Preferences and Response to cis-Zeatin. *Plant Physiol.* **134**:
1102 1654–1661.
- 1103 **Zhao, Y.** (2008). The role of local biosynthesis of auxin and cytokinin in plant
1104 development. *Curr. Opin. Plant Biol.* **11**: 16–22.
- 1105 **Zhou, Z., Sun, L., Zhao, Y., An, L., Yan, A., Meng, X., and Gan, Y.** (2013). Zinc Finger
1106 Protein 6 (ZFP6) regulates trichome initiation by integrating gibberellin and
1107 cytokinin signaling in Arabidopsis thaliana. *New Phytol.* **198**: 699–708.

1109

1110 FIGURE LEGENDS

1111

1112 **Figure 1.** *Hsf1* mutants alter leaf patterning and are caused by missense mutations
1113 in the *ZmHK1* cytokinin receptor. **(A)** Adaxial view of half-leaves from WT and *Hsf1*-
1114 *1603/+* sibs showing the proximal-distal organization of the sheath (s), ligule (l), auricle
1115 (a) and blade (b) and a prong outgrowth (red triangle). Bar = 5 cm. **(B)** Close-up of a
1116 blade margin (b) from WT and *Hsf1*-*1603/+* showing a prong consisting of proximal leaf
1117 segments – sheath (s), ligule (l) and auricle (a) juxtaposed to the blade (b). Bar = 1 cm.
1118 **(C)** Comparison of leaf phenotypes between the three *Hsf1* alleles. L4 (top), 4th leaf
1119 below tassel; L5 (bottom, 5th leaf below tassel. Bar = 10 cm. **(D)** Amino acid alignment
1120 of a portion of the CHASE domain from different plant his-kinase cytokinin receptors
1121 and the three *Hsf1* mutant alleles. Missense residues are marked by black triangles for
1122 the *Hsf1* alleles and by a white triangle for the *Lotus snf2* allele. Amino acid sequences
1123 derived from AT2G01830 (*AHK4*), AM287033 (*LHK1* and *LHK1-snf2*), XM_003570636
1124 (*BdHK1*), XM_002454271 (*SbHK1*), NM_001111389 (*ZmHK1-NCBI*),
1125 GRMZM2G151223 (*ZmHK1-MaizeGDB*), *ZmHK1* from the A619 inbred (*ZmHK1*-
1126 *AEWL*) and the Mo17 inbred (*ZmHK1*-*1603* and *ZmHK1*-*1595*). **(E)** *ZmHK1* receptors
1127 with *Hsf1* mutations show CK independent growth in a yeast his-kinase signaling assay.
1128 Growth of *S. cerevisiae sln* Δ mutant transformed with an empty vector, the *ZmHK1*
1129 vector or one of the *Hsf1* mutant *ZmHK1* vectors on glucose media with no CK (DMSO)
1130 or supplemented with different cytokinins - iP, tZ, or cZ. Growth on galactose media of
1131 the *sln* Δ mutant transformed with each of the assayed vectors. DMSO, dimethyl
1132 sulfoxide; iP, *N*⁶-(Δ^2 -isopentenyl)adenine; tZ, *trans*-zeatin; cZ, *cis*-zeatin. Dilutions of
1133 yeast cultures (O.D.₆₀₀ = 1.0) for each yeast strain are noted on the left of each image.
1134 **(F)** Ribbon diagram of the *ZmHK1* CHASE domain with the *Hsf1* mutations (magenta)
1135 noted and one molecule of *N*⁶-(Δ^2 -isopentenyl)adenine (blue and aqua) complexed in
1136 the binding pocket. Arginine 192 (blue), in the loop domain (red) forming one face of

1137 the binding cavity, is predicted to form a salt bridge with E236, the residue altered in
1138 *Hsf1-1603*. *Hsf1-1595* is P190L, *Hsf1-1603* is E236K and *Hsf1-AEWL* is L238F.

1139

1140 **Figure 2.** Exogenous CK treatment phenocopies the *Hsf1* leaf development defects
1141 and enhances the *Hsf1* mutation. (A) Phenotype of 3-week old wild type and
1142 heterozygous *Hsf1-1603/+* seedlings. Bar = 2 cm. (B) Phenotypes of 3-week old B73
1143 water (- CK) and 10 μ M 6-BAP treated (+ CK) seedlings. Bar = 2 cm. (C) Boxplots of
1144 leaf sizes comparing wild type (WT) to *Hsf1-1603/+* sib seedlings, and B73 water (- CK)
1145 and 10 μ M 6-BAP treated (+ CK) seedlings. Horizontal bars represent the maximum,
1146 third quantile, median, first quantile, and minimum values respectively, dots outside of
1147 the plot are outliers, and the * indicates a *P*-value ≤ 0.0001 calculated from a two-tailed
1148 Student's t-test. (D) Macrohair production on the abaxial sheath and auricle (white
1149 triangles) of 2-week old B73 water (- CK) and 10 μ M 6-BAP treated (+ CK) seedlings.
1150 Insets show an adaxial view of the sheath-blade boundary of leaf 1. (E) Glue
1151 impressions of adaxial leaf 1 blade from 2-week old B73 water (- CK) and 10 μ M 6-BAP
1152 treated (+ CK) seedlings showing increased macrohair presence in the medial blade
1153 and at the margin. (F) CK-induced prong formation in B73 seedlings ($n \geq 12$ for each
1154 treatment). (G) Effect of CK treatment on prong formation in 2-week old *Hsf1-1603/+*
1155 seedlings (yellow arrows mark prongs). Bar = 2 cm. (H) Frequency and leaf number
1156 where the first prong formed in *Hsf1-1603/+* with (red) and without (blue) 10 μ M 6-BAP
1157 treatment ($n \geq 12$ for each treatment). (I) Close-up of prongs formed on leaf 4 from CK-
1158 treated and control *Hsf1-1603/+* seedlings (in [G]). (J) Macrohair production on 2-week
1159 old seedlings due to CK treatment or *Hsf1-1603/+* mutation or both.

1160

1161 **Figure 3.** Expression of CK signaling and responsive genes. (A) Relative mRNA
1162 accumulation of CK genes in different tissues of 2-week old seedlings of the three *Hsf1*
1163 alleles and WT sibs measured by qPCR. For each genotype, values are the means
1164 (\pm SE) of three biological replicates consisting of tissue pooled from at least 3 plants. .

1165 Asterisks indicate significant differences between WT and *Hsf1/+* sib (Student's *t* test, *P*
1166 ≤ 0.05). GL – Green leaf, IL – immature leaf, SA –shot apex. **(B)** Pattern of *ZmHK1* and
1167 *ZmRR3* transcript accumulation in WT and *Hsf1-1603/+* shoot apex. Longitudinal and
1168 transverse sections were hybridized with *ZmHK1* or *ZmRR3* specific antisense probes.
1169 The longitudinal section of *ZmRR3* hybridized to WT is not medial and so *ZmRR3*
1170 expression appears to be apically localized, but it is not. Initiating leaf primordia (yellow
1171 arrows) and leaf primordia margins (red triangles) are marked in the *Hsf1/+* sections
1172 probed with *ZmRR3*. Bar = 30 μm .

1173

1174 **Figure 4.** The *Hsf1* phenotype is enhanced by loss of *ZmRR3* function. **(A)**
1175 Phenotypes of 30-day old (left to right) WT, *abph1/abph1*, *Hsf1-1603/+*, and *Hsf1-*
1176 *1603/+*, *abph1/abph1* mutants. This family segregated 9 wild type, 12 *abph1/abph1*, 10
1177 *Hsf1-1603/+*, and 15 double *Hsf1-1603/+*, *abph1/abph1*, which fits a 1:1:1:1 expected
1178 ratio. Inset shows a close-up of a double *Hsf1*, *abph1* mutant. Bar = 15 cm. **(B)**
1179 Phenotypes of 60-day old plants segregating the same four genotypes in **(A)**. Bar = 10
1180 cm. Insets in the double mutant images show close-ups of prongs from that genotype.
1181 Yellow and red arrowheads mark paired leaves on the *abph1* mutant and prongs on the
1182 *Hsf1/+* mutant, respectively.

1183

1184

1185

1186 **Supplemental Data**

1187

1188 **Supplemental Figure 1.** *Hsf1* phenotypes.

1189 **Supplemental Figure 2.** Prong formation is patterned in *Hsf1* leaves.

1190 **Supplemental Figure 3.** ZmHK1 activity in heterologous yeast his-kinase assay.

1191 **Supplemental Figure 4.** Comparison of ligand binding affinity constants of wild type
1192 and mutant ZmHK1 receptors.

1193 **Supplemental Figure 6.** Effects of CK treatment on leaf growth.

1194 **Supplemental Table 1.** Mature plant phenotypes of the three *Hsf1* alleles.

1195 **Supplemental Table 2.** Frequency of prongs for the three *Hsf1* alleles by leaf position in the
1196 upper shoot..

1197 **Supplemental Table 3:** Primers used for positional cloning or genotyping

1198 **Supplemental Table 4.** Primers used for expression analysis

1199

1200 **Tables**

1201

1202 **Table 1. Apparent affinity constants K_D^* for wild type and mutant ZmHK1**
1203 **receptors with different cytokinins**

K_D^* for cytokinins (nM)									
Assay	Receptor	iP	BA	tZ	cZ	Kin	TD	DZ	Ade
Bacterial spheroplasts	ZmHK1	2.90	3.69	31.8	37.5	33.0	37.6	312.0	>10000
	<i>AEWL</i>	0.36	0.56	6.38	5.56	7.62	93.7	61.6	>10000
	<i>1603</i>	0.59	0.91	7.27	6.74	7.50	111.0	88.0	>10000
Tobacco membrane	ZmHK1	0.52	1.42	7.16	8.31	-	49.2	114.0	>10000
	<i>1595</i>	0.23	0.31	1.65	2.14	-	71.9	14.1	>10000

1204 iP, N^6 -(Δ^2 -isopentenyl)adenine; BA, 6-benzylaminopurine; tZ, *trans*-zeatin; cZ, *cis*-
1205 zeatin; Kin, kinetin; TD, thidiazuron; DHZ, dihydrozeatin, Ade, adenine.

1206

1207

1208

1209

1210

1211

1212

1213

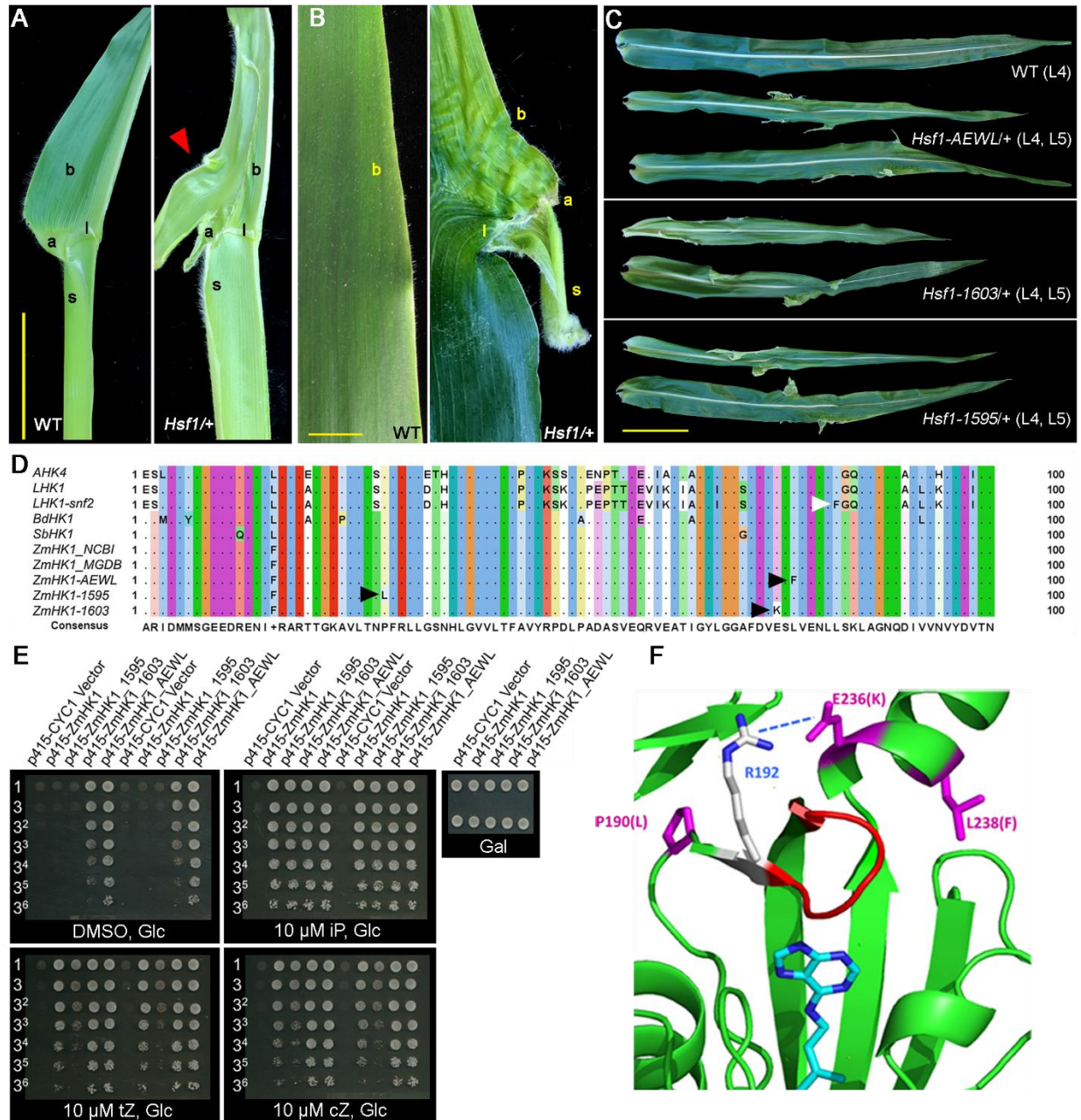
1214 **Table 2. Fold increase of affinity to various cytokinins of mutant receptors**
1215 **compared to ZmHK1**

Cytokinin	Receptor		
	ZmHK1- AEWL	ZmHK1- 1603	ZmHK1- 1595
iP	8.06	4.92	2.26
BA	6.59	4.05	4.58
tZ	4.98	4.37	4.34
cZ	6.74	5.56	3.88
Kin	4.33	4.40	-
TD	0.4	0.39	0.68
DZ	5.06	3.55	8.09
Assay	Bacterial spheroplasts		Tobacco membrane

1216 iP, N^6 -(Δ^2 -isopentenyl)adenine; BA, 6-benzylaminopurine; tZ, *trans*-zeatin; cZ, *cis*-
1217 zeatin; Kin, kinetin; TD, thidiazuron; DHZ, dihydrozeatin, Ade, adenine.

1218

1219



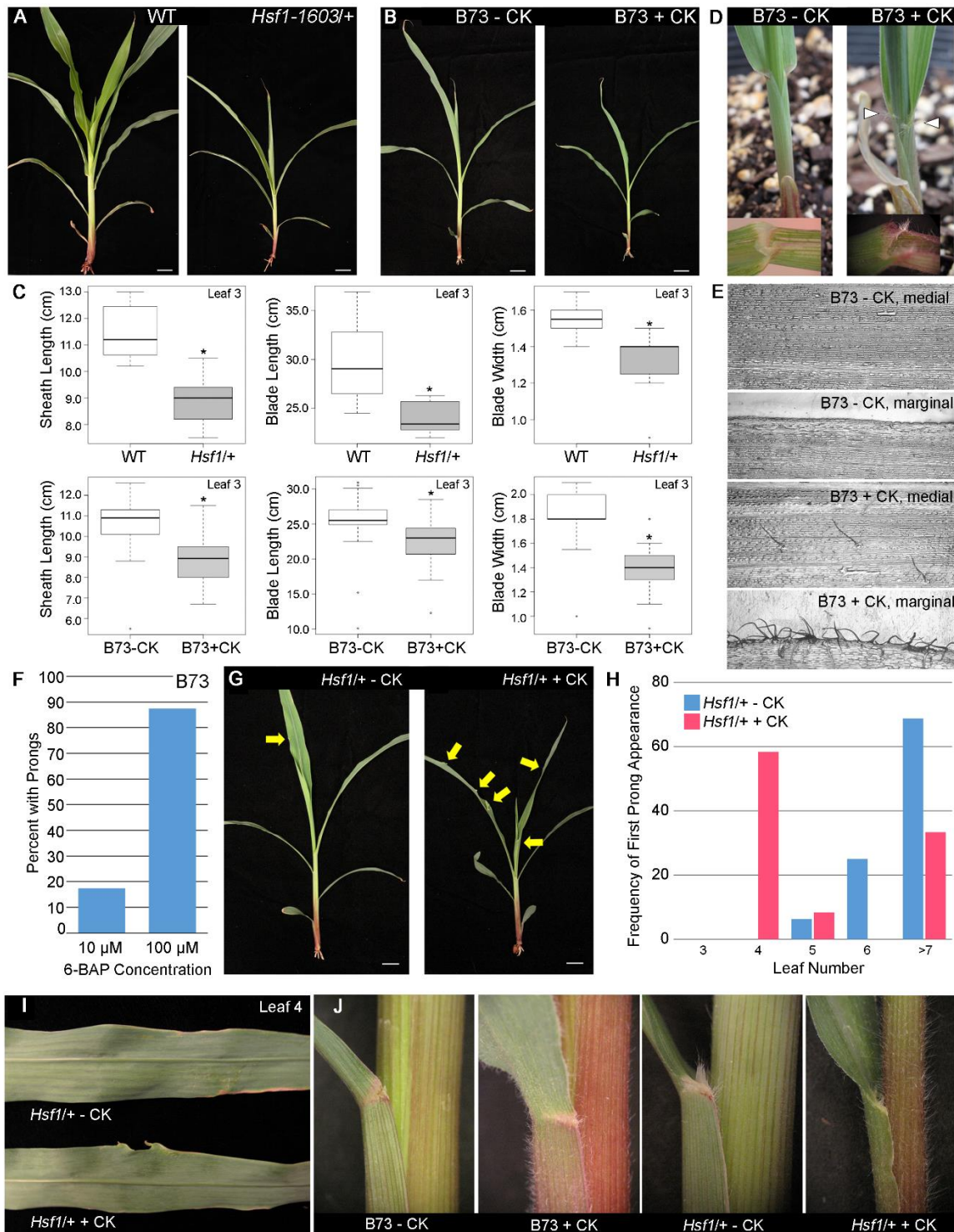
1220
1221

1222 **Figure 1.** *Hsf1* mutants alter leaf patterning and are caused by missense mutations
1223 in the *ZmHK1* cytokinin receptor. **(A)** Adaxial view of half-leaves from WT and *Hsf1*-
1224 *1603/+* sibs showing the proximal-distal organization of the sheath (s), ligule (l), auricle
1225 (a) and blade (b) and a prong outgrowth (red triangle). Bar = 5 cm. **(B)** Close-up of a
1226 blade margin (b) from WT and *Hsf1-1603/+* showing a prong consisting of proximal leaf
1227 segments – sheath (s), ligule (l) and auricle (a) juxtaposed to the blade (b). Bar = 1 cm.
1228 **(C)** Comparison of leaf phenotypes between the three *Hsf1* alleles. L4 (top), 4th leaf
1229 below tassel; L5 (bottom, 5th leaf below tassel). Bar = 10 cm. **(D)** Amino acid alignment
1230 of a portion of the CHASE domain from different plant his-kinase cytokinin receptors
1231 and the three *Hsf1* mutant alleles. Missense residues are marked by black triangles for

1232 the *Hsf1* alleles and by a white triangle for the *Lotus snf2* allele. Amino acid sequences
1233 derived from AT2G01830 (*AHK4*), AM287033 (*LHK1* and *LHK1-snf2*), XM_003570636
1234 (*BdHK1*), XM_002454271 (*SbHK1*), NM_001111389 (*ZmHK1-NCBI*),
1235 GRMZM2G151223 (*ZmHK1-MaizeGDB*), *ZmHK1* from the A619 inbred (*ZmHK1-*
1236 *AEWL*) and the Mo17 inbred (*ZmHK1-1603* and *ZmHK1-1595*). **(E)** *ZmHK1* receptors
1237 with *Hsf1* mutations show CK independent growth in a yeast his-kinase signaling assay.
1238 Growth of *S. cerevisiae sln* Δ mutant transformed with an empty vector, the *ZmHK1*
1239 vector or one of the *Hsf1* mutant *ZmHK1* vectors on glucose media with no CK (DMSO)
1240 or supplemented with different cytokinins - iP, tZ, or cZ. Growth on galactose media of
1241 the *sln* Δ mutant transformed with each of the assayed vectors. DMSO, dimethyl
1242 sulfoxide; iP, *N*⁶-(Δ^2 -isopentenyl)adenine; tZ, *trans*-zeatin; cZ, *cis*-zeatin. Dilutions of
1243 yeast cultures (O.D.₆₀₀ = 1.0) for each yeast strain are noted on the left of each image.
1244 **(F)** Ribbon diagram of the *ZmHK1* CHASE domain with the *Hsf1* mutations (magenta)
1245 noted and one molecule of *N*⁶-(Δ^2 -isopentenyl)adenine (blue and aqua) complexed in
1246 the binding pocket. Arginine 192 (blue), in the loop domain (red) forming one face of
1247 the binding cavity, is predicted to form a salt bridge with E236, the residue altered in
1248 *Hsf1-1603*. *Hsf1-1595* is P190L, *Hsf1-1603* is E236K and *Hsf1-AEWL* is L238F.

1249
1250
1251
1252
1253
1254
1255

1256



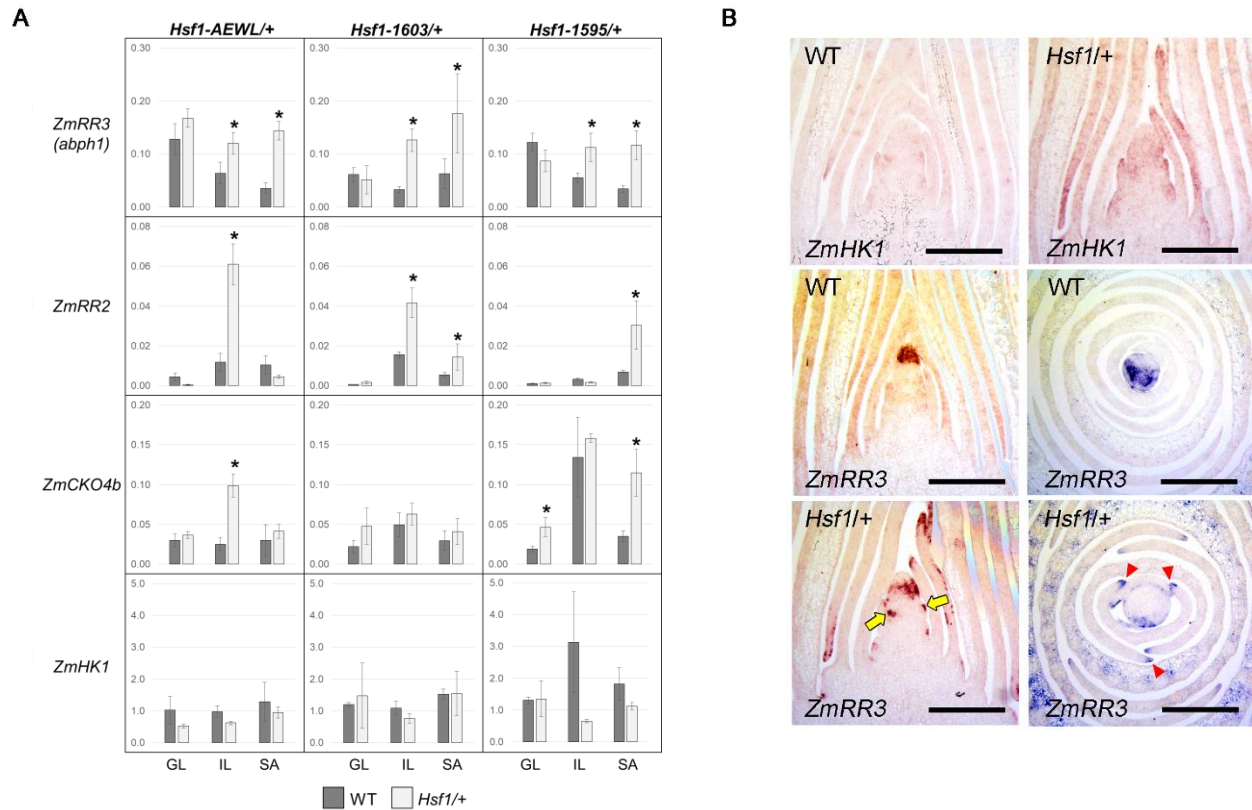
1257
1258

1259 **Figure 2.** Exogenous CK treatment phenocopies the *Hsf1* leaf development defects
1260 and enhances the *Hsf1* mutation. **(A)** Phenotype of 3-week old wild type and
1261 heterozygous *Hsf1-1603/+* seedlings. Bar = 2 cm. **(B)** Phenotypes of 3-week old B73
1262 water (- CK) and 10 μ M 6-BAP treated (+ CK) seedlings. Bar = 2 cm. **(C)** Boxplots of

1263 leaf sizes comparing wild type (WT) to *Hsf1-1603/+* sib seedlings, and B73 water (- CK)
1264 and 10 μ M 6-BAP treated (+ CK) seedlings. Horizontal bars represent the maximum,
1265 third quantile, median, first quantile, and minimum values respectively, dots outside of
1266 the plot are outliers, and the * indicates a *P*-value ≤ 0.0001 calculated from a two-tailed
1267 Student's t-test. (D) Macrohair production on the abaxial sheath and auricle (white
1268 triangles) of 2-week old B73 water (- CK) and 10 μ M 6-BAP treated (+ CK) seedlings.
1269 Insets show an adaxial view of the sheath-blade boundary of leaf 1. (E) Glue
1270 impressions of adaxial leaf 1 blade from 2-week old B73 water (- CK) and 10 μ M 6-BAP
1271 treated (+ CK) seedlings showing increased macrohair presence in the medial blade
1272 and at the margin. (F) CK-induced prong formation in B73 seedlings ($n \geq 12$ for each
1273 treatment). (G) Effect of CK treatment on prong formation in 2-week old *Hsf1-1603/+*
1274 seedlings (yellow arrows mark prongs). Bar = 2 cm. (H) Frequency and leaf number
1275 where the first prong formed in *Hsf1-1603/+* with (red) and without (blue) 10 μ M 6-BAP
1276 treatment ($n \geq 12$ for each treatment). (I) Close-up of prongs formed on leaf 4 from CK-
1277 treated and control *Hsf1-1603/+* seedlings (in [G]). (J) Macrohair production on 2-week
1278 old seedlings due to CK treatment or *Hsf1-1603/+* mutation or both.

1279
1280
1281
1282
1283
1284
1285
1286

1287



1288

1289

Figure 3. Expression of CK signaling and responsive genes. **(A)** Relative mRNA accumulation of CK genes in different tissues of 2-week old seedlings of the three *Hsf1* alleles and WT sibs measured by qPCR. For each genotype, values are the means (\pm SE) of three biological replicates consisting of tissue pooled from at least 3 plants. Asterisks indicate significant differences between WT and *Hsf1*+ sib (Student's *t* test, $P \leq 0.05$). GL – Green leaf, IL – immature leaf, SA –shot apex. **(B)** Pattern of *ZmHK1* and *ZmRR3* transcript accumulation in WT and *Hsf1-1603/+* shoot apex. Longitudinal and transverse sections were hybridized with *ZmHK1* or *ZmRR3* specific antisense probes. The longitudinal section of *ZmRR3* hybridized to WT is not medial and so *ZmRR3* expression appears to be apically localized, but it is not. Initiating leaf primordia (yellow arrows) and leaf primordia margins (red triangles) are marked in the *Hsf1*+ sections probed with *ZmRR3*. Bar = 30 μ m.

1302

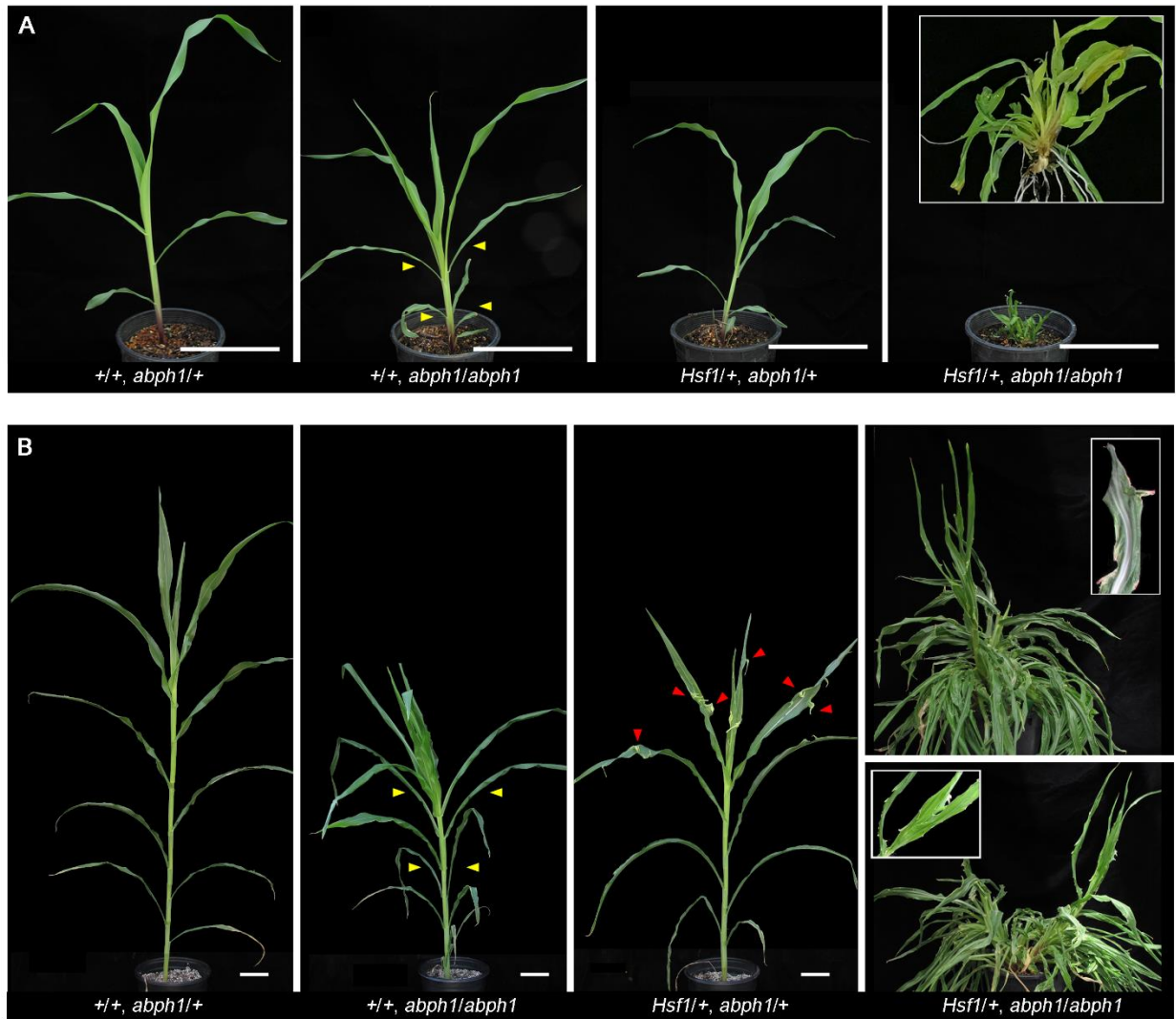
1303

1304

1305

1306

1307



1308

1309

1310 **Figure 4.** The *Hsf1* phenotype is enhanced by loss of *ZmRR3* function. (A)
1311 Phenotypes of 30-day old (left to right) WT, *abph1/abph1*, *Hsf1-1603/+*, and *Hsf1-*
1312 *1603/+*, *abph1/abph1* mutants. This family segregated 9 wild type, 12 *abph1/abph1*, 10
1313 *Hsf1-1603/+*, and 15 double *Hsf1-1603/+*, *abph1/abph1*, which fits a 1:1:1:1 expected
1314 ratio. Inset shows a close-up of a double *Hsf1*, *abph1* mutant. Bar = 15 cm. (B)
1315 Phenotypes of 60-day old plants segregating the same four genotypes in [A]. Bar = 10
1316 cm. Insets in the double mutant images show close-ups of prongs from that genotype.
1317 Yellow and red arrowheads mark paired leaves on the *abph1* mutant and prongs on the
1318 *Hsf1/+* mutant, respectively.

1319

1320

1321